Research Activities in NTT Basic Research Laboratories

Volume 17

Fiscal 2006

September 2007

NTT Basic Research Laboratories,

Nippon Telegraph and Telephone Corporation (NTT)

http://www.brl.ntt.co.jp/

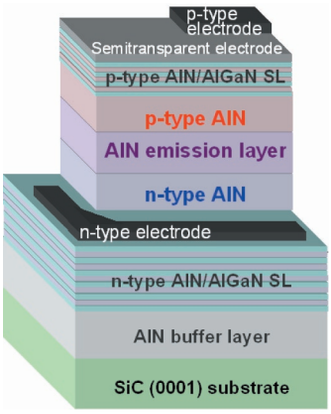

LED structure

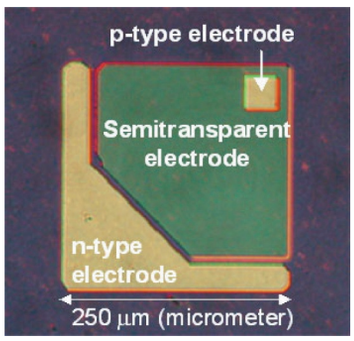

Top view of LED

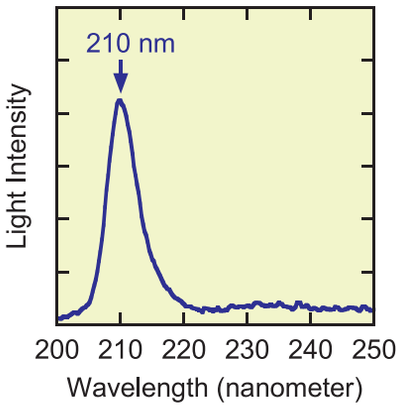

Ultraviolet light emission from LED

Aluminum Nitride Light-Emitting Diodes with the Shortest Wavelength

Aluminum nitride (AlN) is a direct-bandgap semiconductor with a bandgap energy of 6 eV, the largest among semiconductors, and is therefore promising for light-emitting devices with the shortest wavelength for semiconductors. Recently, we have succeeded in p-type and n-type doping of AlN, and have fabricated a p-n homojunction AlN light-emitting diode (LED). (Page 16)

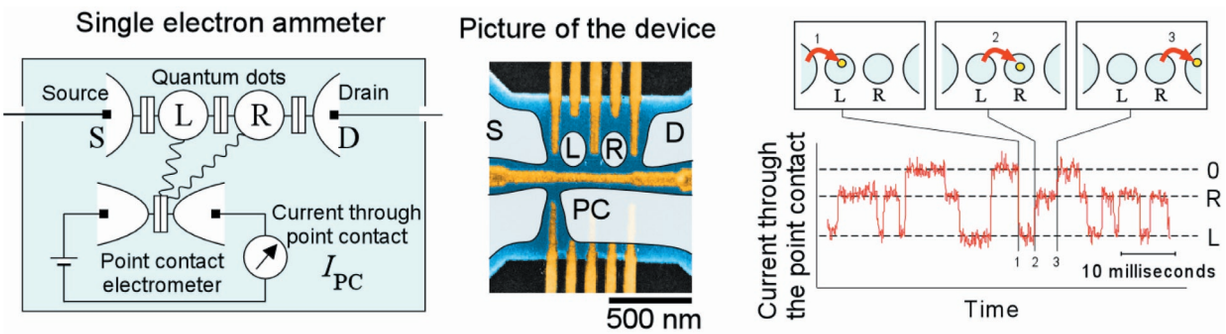

Single-electron Counting Device (Single-electron Ammeter)

A single-electron counting device for detecting individual electron flow in an electric current has been developed. Quantum dots (L and R in the figure) and a point contact electrometer are integrated in a compound semiconductor device, which allows us to measure the location of an electron passing through the quantum dots. The current through the point contact shows three-level fluctuations as shown in the right panel, from which each electron motion (tunneling event) is identified. The device works as an ultimate current meter with single-electron sensitivity. (Page 32)

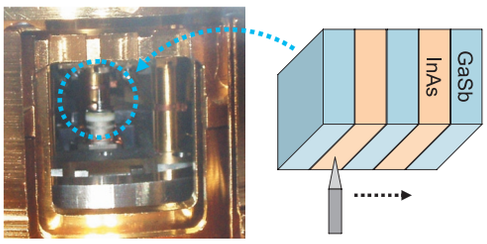

Scanning tunneling spectroscopy on cleaved semiconductor heterostructure surfaces

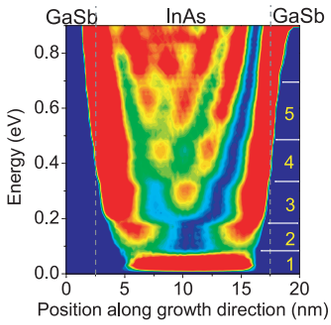

Quantized subbands in a quantum well

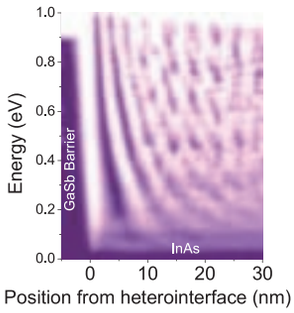

Electron wave interference at a potential barrier

Density-of-states Imaging in Semiconductor Heterostructures

We have succeeded in the spatial imaging of the density-of-states (corresponding to the squared wavefunctions) in semiconductor heterostructures by scanning tunneling spectroscopy on cleaved surfaces. Quantized subbands in a quantum well, electron wave interference at a potential barrier, and wavefunction coupling in a double quantum well have been clearly observed. This method makes it possible to analyze wavefunction distributions in optical and electronic heterostructure devices. (Page 33)

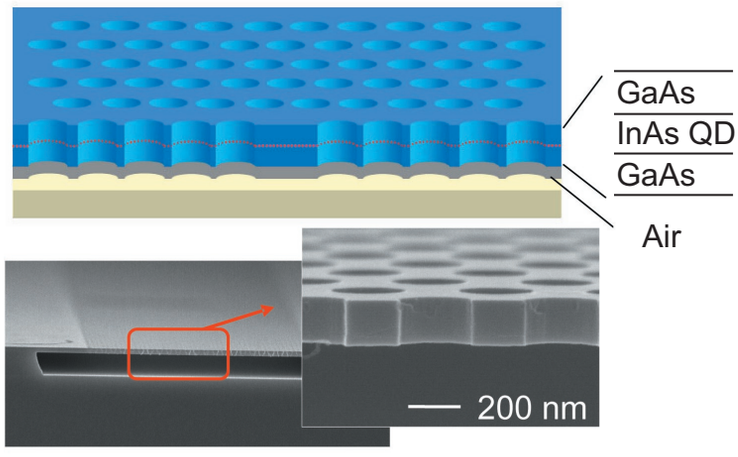

2D photonic crystal slab structure with quantum dots

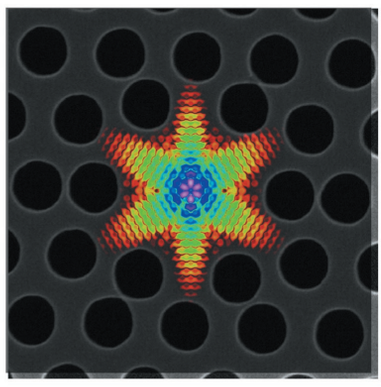

SEM image of nanocavity and calculated electromagnetic field

Quantum Dot Laser Using Photonic Crystal Nanocavity

Ultra low threshold lasing was achieved in quantum dots embedded in a photonic crystal nanocavity. Until now, the processing accuracy of compound semiconductors has been lower than that of silicon, and the absorption characteristic had a detrimental effect on the optical confinement of the cavity. We have greatly improved the dry etching process, and designed the structure to suppress the re-absorption effect. As a result, most of the spontaneous emission of the quantum dots couples with the lasing mode, and this leads to ultra low threshold lasing. (Page 43)

From Science to Innovative Technology

We at NTT Basic Research Laboratories (BRL) are extremely grateful for your interest and support with respect to our research activities.

The missions of BRL are 1) to create new concepts and guiding principles for network and information-processing technologies that will allow us to overcome capacity and security related limitations, and 2) to extend our knowledge of the science and technology that will lead to medium and long-term innovations. We believe that this will both contribute to the success of NTT's business and promote advances in science that will ultimately benefit all mankind. To achieve these goals, we must continuously deliver research output in a timely and well-directed manner. To this end, we adopt a three-tier research theme classification with appropriate management strategies tailored for each:

- *High-priority research*: Work where speed is critically important and that is generally pursued as strategic projects in collaboration with in-house or outside partners.
- *Exploratory research*: Exploratory work that is likely to evolve into high-priority research projects.
- *Innovative research*: Work that goes beyond conventional technology to achieve fundamental and innovative breakthroughs.

BRL's high-priority research themes are currently focused on quantum information processing and nano-bio research. The former aims at clarifying the nature of electrons and photons, which are the basis for the quantum mechanics of light and matter. The goal is to develop practical applications such as quantum cryptography and quantum computing to overcome capacity and security limitations. By exploiting our expertise in quantum optics, quantum solid-state physics, nano-fabrication, and other key technological areas, BRL has achieved remarkable successes in unraveling the mysteries that lie behind a variety of systems including quantum dots, superconducting devices, and cold atoms. Based on these achievements, we are examining the practical viability of quantum cryptography and quantum computers in collaboration with many research institutes, both in Japan and overseas. The aim of our nano-bio research is to create a new area of science through the fusion of neuroscience, biomolecular science, and nanotechnology. This should enable the realization of novel devices that integrate molecular structures, proteins, and artificial nanostructures.

As an example of exploratory researches, one project is investigating quantized mechanical motion in nanometer scale structures together with their quantum electronic properties. BRL researchers are also undertaking exploratory work on techniques that will allow us to manipulate nanostructures at will. These techniques include a method for cutting carbon nanotubes at desired points. Researchers working on spintronics are seeking better

understanding and control of electron spin states with a view to achieving revolutionary developments.

Lastly, we are also pursuing highly innovative research that has the groundbreaking potential to overturn conventional technologies in the near future. The great progress made on wide-bandgap semiconductors, single-electron devices, photonic crystals, and carbon thin films convinces us that they will ultimately displace existing technologies.

To conduct these research activities, BRL is collaborating with many universities and research institutes in Japan, US, Europe, and Asia as well as other NTT laboratories. BRL also regularly organizes international symposia and conferences at NTT Atsugi R&D Center. In February 2007, we hosted the International Conference on Nanoelectronics, Nanostructures and Carrier Interactions, which attracted the participation of more than 140 researchers from around the world. It gives us immense pleasure to fulfill our mission of being an open laboratory in this way, and to disseminate our research output throughout the world.

This report highlights the main achievements and research activities of NTT Basic Research Laboratories in 2006. We hope that it will help to promote awareness of the work undertaken at NTT BRL, and enhance future collaboration.

Junji Yumoto

Director

NTT Basic Research Laboratories

3-1 Morinosato Wakamiya, Atsugi,

Kanagawa 243-0198, Japan

Phone: +81 46 240 3300

Fax : +81 46 270 2358

Contents

Cover photograph:

Long Time Photon Caging by Ultrahigh Q Photonic Crystal Optical Nanocavity

Light is fundamentally difficult to confine or stop in a small space. We succeeded to store photons for an extremely long 1 ns in a very small space by using photonic crystal nanocavity. At the center of the image, a scanning electron microscope image of the ultrahigh Q photonic crystal optical nanocavity is shown, and the electrical field of the trapped photons in a cavity is illustrated at the bottom left.

Member List

As of March 31, 2007
(*/ left NTT BRL in the middle of the year)

NTT Basic Research Laboratories

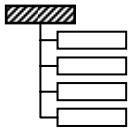

Director, **Dr. Junji Yumoto**

Research Planning Section

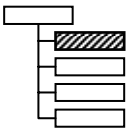

Executive Research Scientist, **Dr. Itaru Yokohama**

Senior Research Scientist, Dr. Hideki Gotoh

Senior Research Scientist, Dr. Koji Muraki

Senior Research Scientist, Supervisor, Dr. Yuichi Harada

NTT R&D Fellow

Prof. Yoshihisa Yamamoto
(Stanford University, U.S.A)
Dr. Hideaki Takayanagi
(Tokyo University of Science)

NTT Research Professor

Prof. Masahito Ueda
(Tokyo Institute of Technology)
Dr. Fujio Shimizu
(The University of Electro-Communications)
Prof. Shintaro Nomura
(University of Tsukuba)
Prof. Kyo Inoue
(Osaka University)

Materials Science Laboratory

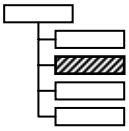

Executive Manager, **Dr. Keiichi Torimitsu**

Dr. Hiroo Omi

Dr. Katsuhiro Ajito Dr. Yuko Ueno
Dr. Isao Tomita Dr. Rakchanok, Rungsawang*

Thin-Film Materials Research Group:

Dr. Toshiki Makimoto (Group Leader)

Dr. Makoto Kasu	Dr. Yasuyuki Kobayashi	Dr. Hisashi Sato*
Dr. Tetsuya Akasaka	Dr. Kazuhide Kumakura	Dr. Shin-ichi Karimoto
Dr. Yoshitaka Taniyasu	Dr. Kenji Ueda	Dr. Atsushi Nishikawa
Dr. Alexandre Tallaire		

Low-Dimensional Nanomaterials Research Group:

Dr. Yoshihiro Kobayashi (Group Leader)

Dr. Fumihiko Maeda	Dr. Hiroki Hibino	Dr. Kawamura Tomoaki*
Dr. Satoru Suzuki	Akio Tokura	Dr. Ilya Sychukov

Molecular and Bio Science Research Group:

Dr. Keiichi Torimitsu (Group Leader)

Dr. Keisuke Ebata	Dr. Kazuaki Furukawa	Dr. Koji Sumitomo
Dr. Nahoko Kasai	Dr. Akiyoshi Shimada	Dr. Hiroshi Nakashima
Dr. Yoshiaki Kashimura	Touichiro Goto	Dr. Tobias Nyberg*
Dr. Mimei Kobayashi*	Dr. Yoichi Shinozaki	Dr. Jonas Rundqvist

Physical Science Laboratory

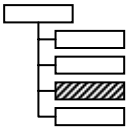

Executive Manager, **Dr. Hiroshi Yamaguchi**
Dr. Yoshiro Hirayama*

Dr. Yukinori Ono

Takeshi Karasawa

Nanodevices Research Group:

Dr. Akira Fujiwara (Group Leader)

Dr. Masashi Uematsu*	Dr. Hiroyuki Kageshima	Dr. Katsuhiko Nishiguchi
Dr. Mohammed Khalafalla		

Nanostructure Technology Research Group:

Dr. Hiroshi Yamaguchi (Group Leader)

Dr. Masao Nagase	Dr. Kenji Yamazaki	Toru Yamaguchi
Junzo Hayashi	Dr. Hajime Okamoto	Dr. Imran Mahboob
Dr. Koji Onomitsu		

Quantum Solid State Physics Research Group:

Dr. Toshimasa Fujisawa (Group Leader)

Dr. Kiyoshi Kanisawa	Dr. Satoshi Sasaki	Dr. Kyoichi Suzuki
Dr. Toshiaki Hayashi	Dr. Takeshi Ohta	Dr. Norio Kumada
Dr. Kei Takashina	Dr. Vincent Renard*	Dr. Paula Giudici

Superconducting Quantum Physics Research Group:

Dr. Kouichi Semba (Group Leader)

Dr. Hayato Nakano	Dr. Tetsuya Mukai	Hirotaka Tanaka
Dr. Shiro Saito	Dr. Kousuke Kakuyanagi	Dr. Ying-Dan Wang
Dr. Alexander Kasper*		

Spintronics Research Group:

Dr. Tatsushi Akazaki (Group Leader)

Dr. Yuichi Harada	Dr. Hiroyuki Tamura	Dr. Yoshiaki Sekine
Dr. Masumi Yamaguchi	Toshiyuki Kobayashi	Dr. Hideomi Hashiba

Optical Science Laboratory

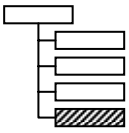

Executive Manager, **Dr. Yasuhiro Tokura**

Dr. Atsushi Yokoo

Quantum Optical State Control Research Group:

Dr. Yasuhiro Tokura (Group Leader)

Dr. Kaoru Shimizu	Kazuhiro Igeta	Masami Kumagai
Dr. Makoto Yamashita	Dr. Hiroyuki Shibata	Dr. Hiroki Takesue
Dr. Fumiaki Morikoshi	Dr. Toshimori Honjo	Dr. Kiyoshi Tamaki
Daisuke Hashimoto	Dr. Jens Tobiska	

Quantum Optical Physics Research Group:

Dr. Hidetoshi Nakano (Group Leader)

Dr. Tetsuomi Sogawa	Dr. Tadashi Nishikawa	Hidehiko Kamada
Dr. Kouta Tateno	Dr. Takehiko Tawara	Dr. Katsuya Oguri
Dr. Atsushi Ishizawa	Dr. Haruki Sanada	Dr. Nicholas Cade*
Dr. Guoquiang Zhang		

Photonic Nano-Structure Research Group:

Dr. Masaya Notomi (Group Leader)

Dr. Satoki Kawanishi	Dr.Eiichi Kuramochi	Dr. Hideaki Taniyama
Dr. Akihiko Shinya	Dr. Masao Kato*	Dr. Takasumi Tanabe
Dr. Heongkyu Ju*		

Distinguished Technical Member

Hiroshi Yamaguchi was born in Osaka on October 30, 1961. He received the B.E., M.S. in physics and Ph.D. degrees in engineering from the Osaka University in 1984, 1986 and 1993, respectively. He joined NTT Basic Research Laboratories in 1986. He was a visiting research fellow in Imperial College, University of London, U.K. during 1995-1996. Since 1986 he has engaged in the study of compound semiconductor surfaces prepared by molecular beam epitaxy mainly using electron diffraction and scanning tunneling microscopy. His current interests are mechanical and elastic properties of semiconductor low dimensional structures. He is a research coordinator of NEDO international joint research project (*Nano-elasticity*) during 2001-2004 and a member of the Japan Society of Applied Physics and the Physical Society of Japan. He was awarded the paper awards of the Japanese Society of Applied Physics in 1989 and 2004. From 2006, he is a guest professor in Tohoku University.

Distinguished Technical Member

Toshimasa Fujisawa was born in Tokyo on May 23, 1963. He received the B.E., M.S. and Ph.D. degrees in electrical engineering from Tokyo Institute of Technology in 1986, 1988 and 1991, respectively. He joined NTT Basic Research Laboratories in 1991. He was a guest scientist in Delft University of Technology, Delft, the Netherlands during 1997-1998. Since 2003, he is also a guest associate professor at Tokyo Institute of Technology. Since 1991 he has engaged in the study of semiconductor fine structures fabricated by focused-ion-beam technique and electron-beam lithography technique, transport characteristics of semiconductor quantum dot. His current interests are single-electron dynamics in quantum dots, and their application to quantum information technologies. He received Sir Martin Wood Prize in 2003 and JSPS (Japan Society for the Promotion of Science) Award in 2005. He is a member of the Japan Society of Applied Physics, and the Physical Society of Japan.

Distinguished Technical Member

Masaya Notomi was born in Kumamoto, Japan, on 16 February 1964. He received his B.E., M.E. and Dr. Eng. degrees in applied physics from University of Tokyo, Tokyo, Japan in 1986, 1988, and 1997, respectively. In 1988, he joined NTT Optoelectronics Laboratories. Since then, his research interest has been to control the optical properties of materials and devices by using artificial nanostructures, and engaged in research on semiconductor quantum wires/dots and photonic crystal structures. He has been in NTT Basic Research Laboratories since 1999, and is currently working on light-propagation control by use of various types of photonic crystals. From 1996-1997, he was with LinköpingUniversity in Sweden as a visiting researcher. He is also a guest associate professor of Tokyo Institute of Technology (2003-). He received 2006/2007 IEEE/LEOS Distinguished Lecturer Award. He is an associate editor of Japanese Journal of Applied Physics. He is a member of the Japan Society of Applied Physics, the American Physical Society, and IEEE/LEOS.

Distinguished Technical Member

Makoto Kasu was born in Tokyo on May 30, 1961. He received the B.E., M.S. and Ph.D. degrees in electrical engineering from Kyoto University in 1985, 1987 and 1990, respectively. He joined NTT Basic Research Laboratories in 1990, and is currently a group leader of Thin-Film Materials Research Group. He was a guest scientist in University of Ulm, Germany from 2002 to 2003. Since 1990 he has engaged in scanning tunneling microscope (STM)-based nanostructure fabrication and widegap semiconductors. His current interests are aluminum nitride (AlN) deep ultraviolet light-emitting diodes (LEDs) and diamond high-frequency high-power transistors. He received Electronic Materials Symposium (EMS) award. He is a member of the Japan Society of Applied Physics, the Institute of Japan, and the Japanese Society of Surface Science. He is also an invited professor of University of Paris (XIII) and the leader of SCOPE project "Diamond RF Power Devices for Microwave, Millimeter-Wave Range Power Amplifiers" of the Ministry of Internal Affairs and Communications, Japan.

Advisory Board (2006 Fiscal Year)

Name	Title Affiliation
Prof. Gerhard Abstreiter	Professor Walter Schottky Institute Germany
Prof. Boris L. Altshuler	Professor Department of Physics Columbia University, U.S.A.
Prof. Serge Haroche	Professor Département de Physique De l'Ecole Normale Supérieure
Prof. Mats Jonson	Professor Department of Physics, Göteborg University, Sweden
Prof. Anthony J. Leggett	Professor Department of Physics University of Illinois at Urbana-Champaign, U.S.A.
Prof. Johan E. Mooij	Professor Kavli Institute of Nanoscience Delft Delft University of Technology, The Netherlands
Prof. John F. Ryan	Professor Clarendon Laboratory University of Oxford, U.K.
Prof. Klaus von Klitzing	Professor Max-Planck-Institut für Festkörperforschung Germany

Invited / Guest Scientists (2006 Fiscal Year)

Name	Affiliation Period
Dr. Akio Tsukada	Tokyo University of Agriculture and Technology, Japan June 05 – March 07
Dr. Go Yusa	Japan Science and Technology Agency (JST), Japan October 05 – September 08
Dr. Yasuyoshi Miyamoto (Interchange Researcher)	NHK Science & Technical Research Laboratories, Japan December 05 – November 06
Prof. Yong-Hang Zhang	Arizona State University, U.S.A. January 06 – July 06
Dr. Goo-Hwan Jeong	Japan Science and Technology Agency (JST), Japan April 06 – July 06
Dr. Yusuke Furukawa	University of Tokyo, Japan May 06 – October 06
Ken Sato	Tohoku University, Japan June 06 – July 06
Assoc. Prof. Shinichi Warisawa	University of Tokyo, Japan June 06 – March 07
Dr. Koji Onomitsu	Waseda University, Japan July 06 – September 06
Dr. Michael Stopa	Harvard University, U.S.A. August 06 – September 06
Dr. Kasper Grove-Rasmussen	University of Copenhagen, Denmark August 06 – December 06
Dr. Yuan-Liang Zhong	Tokyo University of Science, Japan September 06 – February 07

Dr. Yueh-Chin Lin	National Chiao Tung University, Taiwan November 06 – February 07
Assoc. Prof. Takaaki Koga	Hokkaido University, Japan November 06 – December 07
Akira Yamazaki	Meiji University, Japan November 06 – March 08
Dr. Alexandre Kemp	Japan Science and Technology Agency (JST), Japan December 06 – December 07
Prof. Michel Devoret	Yale University, U.S.A. January 07 – February 07
Prof. Amnon Aharony	Ben Gurion University of the Negev, Israel January 07 – April 07
Prof. Ora Entin-Wohlman	Ben Gurion University of the Negev, Israel January 07 – April 07
Dr. Hongwu Liu	Japan Science and Technology Agency (JST), Japan February 07 – January 08

Trainees (2006 Fiscal Year)

Name	Affiliation Period
Simon Perraud	University of Paris 6 / CNRS, France October 04 – September 07
Rebeca Alonso	"Miguel Hernández "University of Elche, Spain January 06 – August 06
Raphael de Gail	ENS (Ecole Normale Supérieure), France February 06 – April 06
Jean-François Morizur	ENS (Ecole Normale Supérieure), France February 06 – July 06
François Parmentier	ENS (Ecole Normale Supérieure), France February 06 – July 06
Benjamin Gaillard	INSA (Institut National des Sciences Appliquées de Toulouse), France February 06 – September 06
Wan-Cheng Zhang	Chinese Academy of Sciences, China February 06 – August 06
Shih-Chieh Huang	National Chiao Tung University, Taiwan R.O.C. March 06 – September 06
Lars Tiemann	Max-Planck-Institut für Festkörperforschung, Germany March 06 – June 06
Christoph Hufnagel	University of Heidelberg, Germany June 06 – June 07
Tiffany Yeh	Rice University, U.S.A. June 06 – August 06

Arthur Goetschy	ESPCI (Ecole Supérieur de Physique et de Chimie Industrielles), France July 06 – December 06
Camille Janer	ESPCI (Ecole Supérieur de Physique et de Chimie Industrielles), France July 06 – December 06
Samir Etaki	Delft University of Technology, The Netherlands September 06 – December 06
Michailas Romanovas	Vilnius Gediminas Technical University, Lithuania January 07 – August 07
Joana Durao	Porto's University, Portugal January 07 – August 07
Ari Siitonen	University of Kuopio, Finland January 07 – August 07
Daan Sprunken	University of Twente, The Netherlands January 07 – August 07
Sylvain Sergent	INSA (Institut National des Sciences Appliquées de Rennes), France January 07 – August 07
Florian Domengie	INSA (Institut National des Sciences Appliquées de Toulouse), France February 07 – September 07
Guillaume Vincent	INSA (Institut National des Sciences Appliquées de Toulouse), France February 07 – September 07

Japanese Students (2006 Fiscal Year)

Name	Affiliation (Period)
Yuichi Igarashi	University of Tokyo, Japan (Apr. 06 – Mar. 07)
Daisuke Itoh	Tohoku University, Japan (June 06 – Mar. 07)
Kenzo Ibano	Keio University, Japan (Apr. 06 – Feb. 07)
Shoko Utsunomiya	University of Tokyo, Japan (Apr. 06－Mar. 07)
Taichi Urayama	Keio University, Japan (Nov. 06 – Mar. 07)
Akihiro Eguchi	Kyushu University, Japan (Sep. 06 – Nov. 07)
Masato Edamoto	University of Tokyo, Japan (June 06 – Mar. 07)
Kuniaki Endo	Tokyo University of Science, Japan (Apr. 06 – Sep. 06)
Akira Oiwa	University of Tokyo, Japan (Apr. 06 – Mar. 07)
Kenichi Ono	University of Tokyo, Japan (July 06 – Aug. 07)
Satoru Ohno	Keio University, Japan (Apr. 06 – Mar. 07)
Minoru Oda	University of Tokyo, Japan (Apr. 06－Mar. 07)
Junya Ono	University of Tsukuba, Japan (Apr. 06 – Mar. 07)
Seiichiro Kagei	Tokyo University of Science, Japan (May 06 – Sep. 06)
Ryo Kajiura	Tokyo Institute of Technology, Japan (Apr. 06 – Mar. 07)
Keiichi Katoh	University of Tokyo, Japan (June 06 – Mar. 07)
Takayuki Kaneko	Meiji University, Japan (Apr. 06 – Mar. 07)
Takehito Kamada	Tohoku University, Japan (May 06 – Mar. 07)
Sunggu Kang	University of Tsukuba, Japan (Apr. 06 – Mar. 07)
Yosuke Kitamura	University of Tokyo, Japan (Apr. 06－Mar. 07)
Kenichiro Kusudo	University of Tokyo, Japan (Aug. 06－Mar. 07)
Christo Buizert	University of Tokyo, Japan (Apr. 06－Mar. 07)
Marika Gunji	Keio University, Japan (Apr. 06 – Aug. 06)
Ryota Koizumi	Tokyo University of Science, Japan (Nov. 06 – Mar. 07)
Daiu Koh	University of Tokyo, Japan (June 06－Mar. 07)

Tetsuo Kodera	University of Tokyo, Japan (Apr. 06 – Mar. 07)
Takashi Kobayashi	Tohoku University, Japan (June 06 – Mar. 07)
Yosuke Sasaki	Tokyo Institute of Technology, Japan (Apr. 06 – Mar. 07)
Jonathan Baugh	University of Tokyo, Japan (Oct. 06 – Mar. 07)
Go Shinkai	Tokyo Institute of Technology, Japan (Apr. 06 – Mar. 07)
Akihiro Souma	University of Tokyo, Japan (Apr. 06 – Mar. 07)
Atsushi Sogabe	Shonan Institute of Technology, Japan (Apr. 06 – Mar. 07)
Hidenobu Takahashi	Toyohashi University of Technology, Japan (Jan. 07 – Feb. 07)
Hiroyuki Takamichi	Tohoku University, Japan (May 06 – Mar. 07)
Naohiro Takemoto	Toyohashi University of Technology, Japan (Jan. 07 – Feb. 07)
Masaya Tazawa	Tokyo University of Science, Japan (Apr. 06 – Mar. 07)
Ryosuke Tanaka	University of Tokyo, Japan (June 06 – Mar. 07)
Koujiro Tamaru	University of Tokyo, Japan (June 06 – Mar. 07)
Shun Chikamori	Tokyo Institute of Technology, Japan (Apr. 06 – Mar. 07)
Shouei Tsuruta	Tokyo University of Science, Japan (Apr. 06 – Mar. 07)
Eigo Totoki	University of Tokyo, Japan (Apr. 06 – Mar. 07)
Hiromasa Nakano	Tokyo University of Science, Japan (Apr. 06 – Mar. 07)
Tomohiro Nakamura	Shonan Institute of Technology, Japan (Apr. 06 – Mar. 07)
Yoshitaka Niida	Tohoku University, Japan (May 06 – Mar. 07)
Yuita Noguchi	Osaka University, Japan (Aug. 06 – Sep. 07)
Keiichiro Nonaka	University of Tokyo, Japan (June. 06 – Mar. 07)
Junichi Hashimoto	Yokohama National University, Japan (Apr. 06 – Mar. 07)
Takuro Hashimoto	Shibaura Institute of Technology, Japan (Oct. 06 – Mar. 07)
Junichiro Hayakawa	Tohoku University, Japan (May 06 – Mar. 07)
Kenichi Hidachi	University of Tokyo, Japan (Aug. 06 – Mar. 07)
Hirotaka Masuyama	Tokyo University of Science, Japan (Oct. 06 – Mar. 07)
Takao Yamaguchi	Tokai University, Japan (Apr. 06 – Mar. 07)
Mizuki Miyamoto	Shonan Institute of Technology, Japan (Apr. 06 – Mar. 07)

Kunio Morita	Tokyo University of Science, Japan (Apr. 06 – Mar. 07)
Noriko Moritake	Nagaoka University of Technology, Japan (Oct. 06 – Feb. 07)
Shin Yabuuchi	Keio University, Japan (Apr. 06 – Mar. 07)
Michihisa Yamamoto	University of Tokyo, Japan (Apr. 06 – Mar. 07)
Takahito Watanabe	Tokyo Institute of Technology, Japan (Aug. 06 – Sep. 06)

Ⅰ. Research Topics

Overview of Research in Laboratories

Material Science Laboratory Keiichi Torimitsu

The Materials Science Laboratory (MSL) aims at producing new functional materials and designing of advanced device based on novel materials and biological function. Controlling the configuration and coupling of atoms and molecules is our approach to accomplish these goals. Bio-nano research is set as our principle research in this laboratory.

We have three research groups covering from semiconductor devices, such as GaN, to organic materials, such as receptor proteins. The characteristic feature of MSL is the effective sharing of the unique nanofabrication and measurement techniques of each group. This enables fusion of research fields and techniques, which leads to innovative material research for the IT society.

We set up European laboratory in U.K. for bio-nano research, our principal research, in last year and strengthen our research activities. We promote collaborations with international organizations to develop a firm basis of basic science.

Physical Science Laboratory Hiroshi Yamaguchi

We are studying solid-state quantum systems and devices, which will have revolutionary impact on communication and information technologies in the 21st century. In particular, we are making firm and steady progress in the pursuit for solid-state nanodevices, and related physics and technology for future quantum information processing. We maintain an open-door policy and engage in collaborations with many outside organizations to enhance our basic research into fundamental issues.

The five groups in our laboratory are working in the following areas: quantum coherent control of semiconductor and superconductor systems, carrier interactions in semiconductor hetero- and nanostructures, spintronics manipulating both electron and nuclear spins, precise and dynamical control of single electrons, nanodevices operating at ultimately low power consumption, atom traps/optics, and novel nanomechanics based on compound semiconductors. These studies are supported by cutting-edge nanolithography techniques, well-controlled nanofabrication processes, high-quality crystal growth, and theoretical studies including first-principle calculations.

Optical Science Laboratory Yasuhiro Tokura

This laboratory aims the development of core-technologies that will innovate on optical communications and optical signal processing, and seeks fundamental scientific progresses.

The three groups in our laboratory are working for the quantum state control of light, the quantum state control of materials by light, the analysis of high speed phenomena using very short pulse laser, the optical properties of nano-structure semiconductor like quantum dot, and very small optical integrated circuit using two-dimensional photonic crystals.

In this year, we realized improvements of quantum cryptography and quantum entangled photon pair generation, high-Q (10,000) compound semiconductor photonic crystal resonator, and measurements of photon decay time and pulse delay time in ultra-high Q-value photonic crystal resonator.

Aluminum Nitride Light-Emitting Diodes with the Shortest Wavelength

Yoshitaka Taniyasu and Makoto Kasu
Materials Science Laboratory

Aluminum nitride (AlN) is a direct-bandgap semiconductor with a bandgap energy of 6 eV, the largest among semiconductors, and is therefore promising for light-emitting devices with the shortest wavelength for semiconductors. Recently, we have succeeded in p-type and n-type doping of AlN and have fabricated a p-n homojunction AlN light-emitting diode (LED) [1].

The AlN layers were epitaxially grown on SiC (0001) substrate by metalorganic vapor phase epitaxy (MOVPE). To improve the crystal quality of the AlN layers, we suppressed the parasitic reaction of Al and N sources in the gas phase. P-type and n-type AlN layers were obtained by Mg and Si doping during MOVPE growth, respectively [1, 2]. Figure 1 shows schematics of the AlN LED. In this LED structure, between the p-type and n-type AlN layers, an undoped AlN emission layer was inserted to suppress Mg- and Si-impurity-related emission from the p-type and n-type AlN layers. The p-type and n-type AlN/AlGaN superlattices (SLs) were used to reduce the contact resistance of the electrodes.

Figure 2 shows the emission spectrum of the AlN LED. Deep-ultraviolet light emission was observed at 210 nm, the shortest wavelength ever reported for any kind of semiconductors. On the basis of optical reflection and cathodoluminescence measurements of free-exciton transition in AlN, we assigned the light emission to a near-band-edge emission from AlN.

Because light with a shorter wavelength has a higher energy, the AlN LEDs can be applied to light sources for decomposing very stable, harmful chemical substances, such as dioxin and polychlorinated biphenyls (PCBs), which cause serious environmental problems all over the world. We will increase the emission efficiency of the AlN LEDs to a practical level by further improving their crystal quality and doping efficiency.

[1] Y. Taniyasu, M. Kasu, and T. Makimoto, Nature **441** (2006) 325.
[2] Y. Taniyasu, M. Kasu, and T. Makimoto, Appl. Phys. Lett. **89** (2006) 182112.

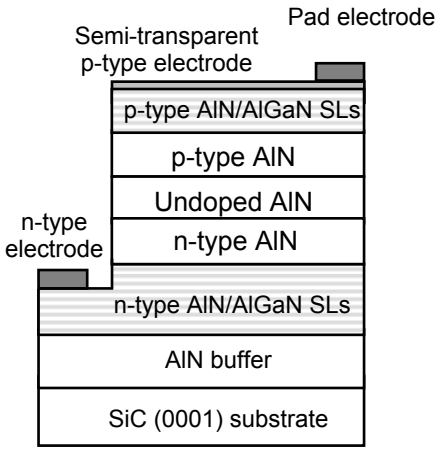

Fig. 1. Device structure of AlN LED.

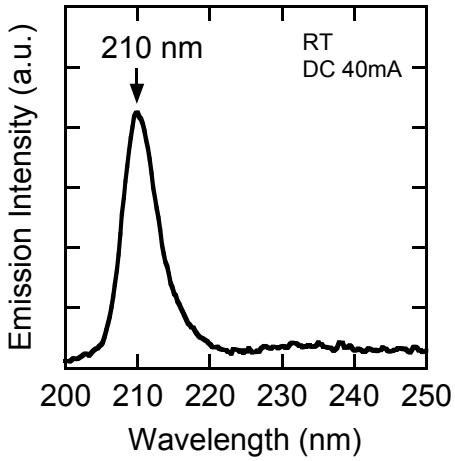

Fig. 2. Emission spectrum of AlN LED.

Diamond FET with Maximum Frequency of Oscillation of 120 GHz

Kenji Ueda and Makoto Kasu
Materials Science Laboratory

Diamond is expected to be the most suitable material for high-power high-frequency electronic devices because of its high electric breakdown field (>10 MV/cm), high carrier mobility (4500 cm^2/Vs for electrons, 3800 cm^2/Vs for holes), and highest thermal conductivity (22 W/cmK). Recently, using homoepitaxial single-crystal CVD diamond, we achieved the maximum output-power density of 2.1 W/mm at 1 GHz [1], which is high enough for power amplifiers of the base stations in wireless communications systems. However, the size of single-crystal CVD diamond is limited to 4 mm, which is the size of commercially available HPHT-synthesized diamond substrates. From the viewpoint of semiconductor-device processing, at least four-inch wafers are needed. One possible solution to this problem is to use high-quality polycrystalline diamond, whose maximum size is 4 inches. Here, using a high-quality polycrystalline diamond film, we report significant progress in fabricating FETs. The grain size of the polycrystalline film is ~100 μm, which is comparable to our FET size. Thus, the effect of the grain boundary seems to be very small.

As shown in Fig. 1, the FETs were fabricated on the freestanding polycrystalline diamond grown by CVD (size: 10 mm × 10 mm × 0.5 mm). The diamond surface was passivated with hydrogen (H-passivation) to form a quasi two-dimensional hole channel. The source and drain Au ohmic contacts were formed on the H-terminated surface. Electron-beam lithography and self-alignment techniques enabled us to form 0.1-μm-long Al Schottky gate contacts. The DC characteristics show drain current (I_{DS}) of 550 mA/mm at gate source voltage (V_{GS}) of -3.5 V. The I_{DS} is comparable to the maximum value of single-crystal CVD diamond FETs. The DC transconductance (g_m) stays high (~140 mS/mm) in a relatively wide V_{GS} range. The transition frequency (f_T) and maximum frequency of oscillation (f_{max}) were extracted from the frequency dependence of the short circuit current gain ($|h21|^2$) and the unilateral power gain (U) as shown in Fig. 2. The maximum f_{max} is 120 GHz, and in a different bias condition, f_T of 45 GHz was obtained. These f_T and f_{max} values are the highest among diamond FETs [2].

[1] M. Kasu, K. Ueda, H. Ye, Y. Yamauchi, et al., Electron. Lett. **41** (2005) 1249.
[2] K. Ueda, M. Kasu, Y. Yamauchi, et al., IEEE Electron Device Lett. **27** (2006) 570.

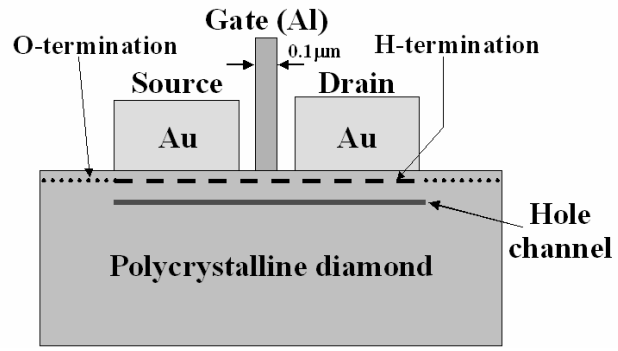

Fig. 1. Schematic cross-section of a polycrystalline diamond FET.

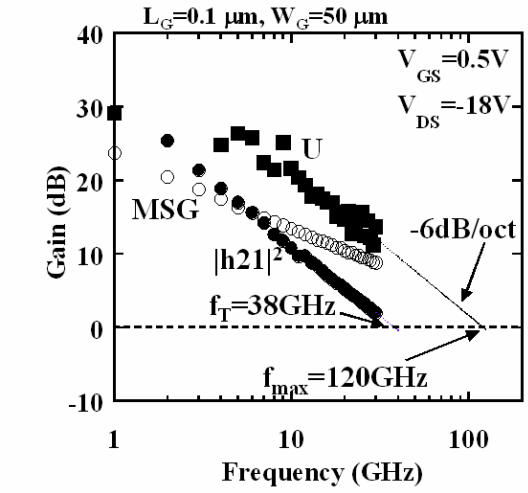

Fig. 2. RF gain plot of FET.

High Breakdown Voltage with Low On-state Resistance of InGaN/GaN Vertical Conducting Diodes

Atsushi Nishikawa, Kazuhide Kumakura, and Toshiki Makimoto
Materials Science Laboratory

Due to wide band gap and high critical electric field of GaN, GaN-based electronic devices are promising for high-power and high-temperature operation. Although a lateral conducting structure using a semi-insulating substrate such as sapphire is usually fabricated for GaN-based devices, a vertical conducting structure using a conductive substrate is advantageous for lower-loss and higher current density. Therefore, GaN-based vertical conducting devices are expected to be preferable for high-power electronic device applications. So far, the study on GaN-based vertical pn junction diode was insufficient because of a high-resistance p-GaN layer and a buffer layer to grow a GaN layer on a hetero-substrate. We have overcome these difficulties by using an InGaN layer for the p-type layer and GaN substrate on which a GaN layer can be directly grown. The diode fabricated in this study exhibits a high breakdown voltage with a low on-state resistance [1].

The samples were grown on n-GaN substrates, using metalorganic vapor phase epitaxy (MOVPE). The sample structure consists of a 1.8-μm or 3.6-μm-thick lightly doped n-GaN layer and a 140-nm-thick p-InGaN layer. For comparison, the same diode structure with 1.8-μm-thick n-GaN was grown on a conductive SiC substrate. Figure 1 shows reverse current-voltage (*I-V*) characteristics. The leakage current of the diode on a GaN substrate is one order of magnitude lower than that on a SiC substrate due to the better crystal quality of GaN grown on a GaN substrate. Since a thick crack-free GaN layer can be grown on a GaN substrate, the breakdown voltage increases with increasing n-GaN layer thickness. For the 3.6-μm-thick GaN layer, the breakdown voltage (V_B) reaches as high as 571 V. At the same time, we obtained the low on-state resistance of 1.23 mΩcm^2 because of absence of the buffer layer, as shown in Fig. 2. The figure-of-merit, V^2/R_{on}, is calculated to be 265 MW/cm^2, which is the highest value among those ever reported for GaN-based vertical conducting Schottky and pn junction diodes.

[1] A. Nishikawa, K. Kumakura, and T. Makimoto, Appl. Phys. Lett. **89** (2006) 153509.

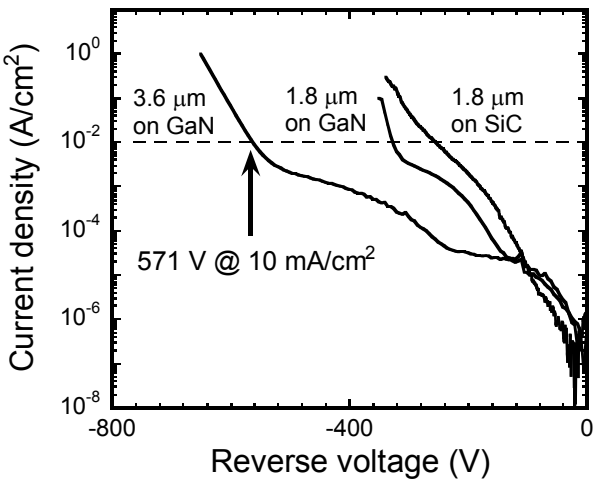

Fig. 1. Reverse *I-V* characteristics.

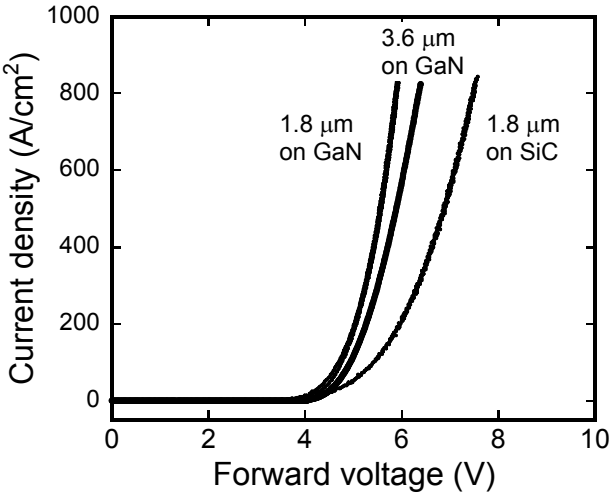

Fig. 2. Forward *I-V* characteristics.

Ultraviolet Luminescence from Hexagonal BN Heteroepitaxial Layers

Yasuyuki Kobayashi, Tetsuya Akasaka, and Toshiki Makimoto
Materials Science Laboratory

Hexagonal boron nitride (h-BN) is a promising material system for exciton-based quantum information processing and for optical device applications in the ultraviolet spectral region. For investigating the optical properties and fabricating optical devices with a p-n junction and quantum well structures, a high-quality h-BN layer on a suitable substrate is indispensable. During the past few decades, BN thin films have been deposited by a number of methods. However, there has been no report of ultraviolet luminescence at room temperature (RT) from these BN thin films.

Recently, we have achieved growth of single crystal h-BN (0001) heteroepitaxial layers on Ni (111) substrate by flow-rate modulation epitaxy (FME) using triethylboron and ammonia (NH_3) [1]. Here, we report RT observation of near-band-gap (NBG) luminescence at a wavelength of 227 nm in cathodoluminescence (CL) from the h-BN heteroepitaxial layers [2].

Figure 1 shows the CL spectra for h-BN layers grown under NH_3 supply times of 1, 2, and 3 s with NH_3 flow rate of 700 sccm. A NBG ultraviolet emission peak centered at energy of 5.47 eV (227 nm) and one broad deep-level emission peak centered at around 3.85 eV (322 nm) are clearly observed for h-BN layer grown under NH_3 supply times of 3 s. To our knowledge, this dominant NBG ultraviolet emission feature at RT has never reported for h-BN films deposited on any substrates. The luminescence intensity at the NBG peak increases monotonically with increasing NH_3 supply time, indicating that h-BN grown by FME with longer NH_3 supply time is preferable for obtaining stronger NBG luminescence.

Figure 2 shows the NH_3 supply time dependence of c-axis lattice constant and full width at half maximum (FWHM) of (0002) h-BN X-ray rocking curve (XRC) for these three h-BN samples. The c-axis lattice constant of all three is identical to that of bulk h-BN samples. The FWHM of the (0002) h-BN XRC decreases from 1.5 to 0.7° with increasing NH_3 supply time from 1 to 3 s. The FWHM of 0.7° is the narrowest value ever reported for a h-BN layer. The lower h-BN growth rate and larger amount of NH_3 with the longer NH_3 supply time may reduce the lattice defects in h-BN heteroepitaxial layers, resulting in the stronger NBG ultraviolet emission from h-BN samples.

The present result is a vital step toward the ultimate goal of h-BN-based optical devices.

[1] Y. Kobayashi, et al., J. Cryst. Growth **298** (2007) 325.
[2] Y. Kobayashi, et al., Phys. Stat. Sol. (b) **244** (2007) 1789.

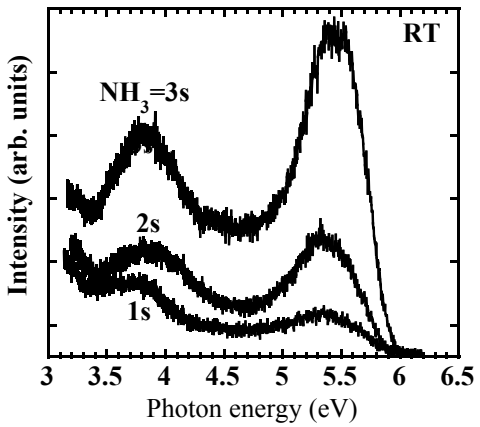

Fig. 1. CL spectra at RT from h-BN thin films grown by FME.

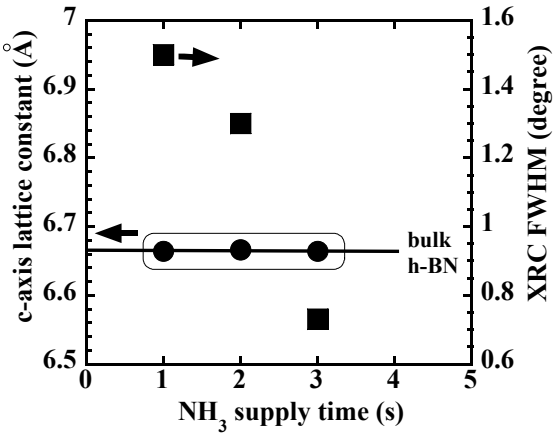

Fig. 2. The lattice constant and the FWHM of XRC as a function of the NH_3 supply time.

Single-walled Carbon Nanotube Synthesis Using Gold, Silver and Copper Nanoparticle Catalysts

Daisuke Takagi[1] and Hiroki Hibino[2]
[1]Tokyo University of Science, [2]Materials Science Laboratory

We succeeded in synthesizing high-quality single-walled carbon nanotubes (SWCNTs) from gold-group elements (Cu, Ag and Au) by chemical vapor deposition (CVD) for the first time [1]. SWCNTs are a key material in nanotechnology and have been intensively studied as the building blocks of nanoelectronics. Iron-group elements (Fe, Co, and Ni) have been used as catalysts for SWCNT synthesis by CVD. However, the detailed role of metal catalyst for the nucleation and growth of SWCNT is not fully understood yet. Our finding should shed new light on the essential role of catalysts in SWCNT growth and should lead to highly controlled SWCNT synthesis by using novel catalyst species.

CVD, in which carbon-containing precursor molecules like ethanol or methane reacts with metal catalyst nanoparticles at elevated temperature, is the most common SWCNT synthesis process being investigated toward practical applications. Iron-group elements and their alloys (Co-Mo, Fe-Co etc) have been mainly used as the catalyst materials for CVD growth. On the other hand, gold-group elements have been regarded as the most unlikely elements to produce SWCNTs since it has been assumed that catalysts must have an affinity for carbon, e.g. high solubility and compound formation. The results of our work (Fig.1) overrule this assumption and indicate that SWCNTs can be formed from gold-group elements, which have extremely low solubility of carbon in bulk phase. The traditional CVD growth mechanism is based on the consideration of the affinity between carbon and catalyst species. In this study, we demonstrated that gold-group elements act as highly efficient catalysts for CVD synthesis of SWCNTs under the following three conditions: (1) Very small metal nanoparticles (3 nm or less in diameter). (2) For activation (Fig. 2), heat-treatment at high temperature (~900 ºC) in air for cleaning of catalyst surfaces. (3) High growth temperature for thermal decomposition of carbon-containing precursor molecules. Moreover, this recipe is also effective for other various metals, such as platinum-group elements (Rh, Pd and Pt), and results in high-density SWCNT yields by CVD. These results mean that the catalytic function for SWCNT synthesis is not specific to the properties of iron-group elements, such as solubility of carbon and precipitation of graphite. Therefore, the CVD growth mechanism from catalyst particles should be reconsidered taking this fact into account. The availability of novel catalyst materials will push the development of growth processes for precise control of SWCNT structures and their non-ferromagnetic properties and catalytic activities for semiconductor nano-wire growth will lead to new applications of SWCNTs in industries.

[1] D. Takagi, et al., Nano Lett. **6** (2006) 2642.

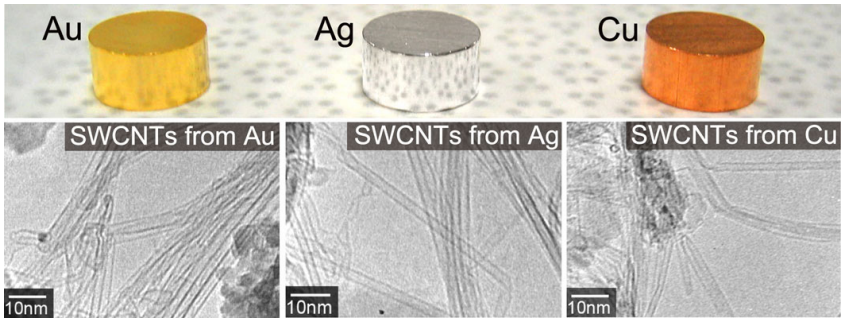

Fig. 1. TEM images of SWCNTs grown from Au, Ag, and Cu catalyst nanoparticles.

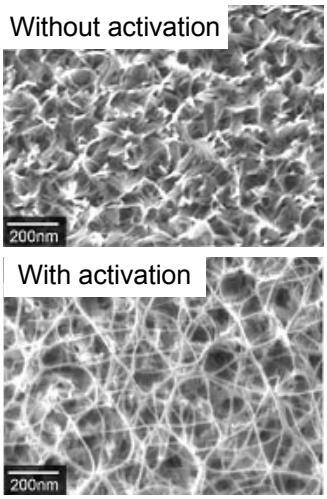

Fig. 2. Comparison of SWCNT yield without and with activation process.

Chemical States of Metal Catalysts in CVD Ambient for Single-walled Carbon Nanotube Growth

Fumihiko Maeda
Materials Science Laboratory

Single-walled carbon nanotubes (SWCNTs) are promising for the generation beyond silicon-based microfabrication technology. However, the mixture of various characteristics, such as metals and semiconductors with various band gaps, are obtained for CNTs. The control of their characteristics is essential in order to achieve large-scale integration for CNT-based devices. Hence, we have been investigating the growth mechanism of CNTs with the aim of controlling their growth and obtaining the desired CNTs. Since catalytic nanoparticles play an important role in growing CNTs, their chemical states are of great interest for this investigation. Recently, we have succeeded in growing SWCNTs by CVD and performing successive *in--situ* x-ray photoelectron spectroscopy measurements. As a result, we have been able to elucidate the chemical state of catalytic nanoparticles after the growth [1, 2].

Figure 1 shows the core-level photoelectron spectra of Co, which is a catalyst for the CNT growth. These spectra were captured before the growth process, at the heating stage, and after CNT growth using ethanol. In the case of *ex-situ* deposition, which is the conventional growth procedure, Co was oxidized by exposure to air, resulting in the formation of Co_3O_4. This oxide turned to CoO during the heating process under ultra-high vacuum and, finally, metallic Co was obtained after CNT growth. In the case of *in-situ* deposition, the new process without air-exposure after metal deposition, Co remained metallic throughout the growth process. These two results indicate that the metallic state is stable under the growth ambient. This is inconsistent with existing CNT growth models, which need the carburization of catalytic nanoparticles. Meanwhile, the CNT yield for the *in-situ* deposition was higher than that for the *ex-situ* deposition. From the analysis of core-level photoelectron intensity, we found that the amount of decomposed carbon on the surface for the *in-situ* deposition is larger than that for the *ex-situ* deposition. The situation after CNT growth in the former case is schematically illustrated in Fig. 2. The formation of thick graphitic films indicates that the uniform metallic nanoparticles have a high ability for the decomposition and that a large amount of migrating carbon remains without being included in the nanoparticles during CVD. We will further investigate the reactions of CNT growth and clarify the growth mechanism.

[1] F. Maeda, et al., Jpn. J. Appl. Phy. **46** (2007) L148.
[2] F. Maeda, et al., Mater. Res. Soc. Symp. Proc. **96** (2007) 30963-Q05-04.

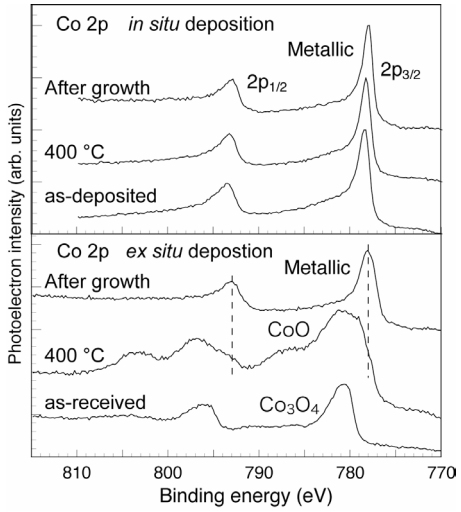

Fig. 1. Co 2p photoelectron spectra.

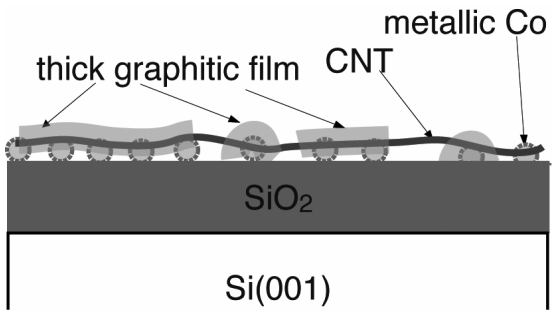

Fig. 2. Schematic representations after CNT growth.

Position Control of Nanowires Using Catalysts Islands Arranged at Surface Atomic Steps

Hiroki Hibino[1] and Kouta Tateno[2]
[1]Materials Science Laboratory, [2]Optical Science Laboratory

Semiconductor nanowires are attracting intense interest as building blocks of future nanoscale electronic and optoelectronic devices. To pursue their application, we have to produce nanowires with controlled size, structure, and position. This is critically related to the control of the metal catalyst used in nanowire formation based on the vapor-liquid-solid mechanism. Gold is one of the most widely used metal catalysts, and we have already shown that the size and position of Au-Si alloy islands can be controlled using atomic steps on Si(111) as templates for island formation [1]. Here, we demonstrate that these islands act as catalysts for the fabrication of vertical GaP nanowires aligned in one dimension [2].

Au-Si alloy islands arranged at atomic steps were obtained by depositing Au on Si(111) at high (~700°C) and then low (~400°C) temperatures. Their size and density were controlled by monitoring the island formation *in-situ* in real time using low-energy electron microscopy. After the Au-Si alloy island formation, the samples were removed from UHV to air and introduced into the metal organic vapor phase epitaxy reactor without any special treatments. We found that there are three aspects to the growth of vertical GaP nanowires on Si(111): co-supply of trimethylgallium and PH_3, two growths at different temperatures, and a low PH_3 flow rate.

Figure 1 shows a scanning electron microscopy (SEM) image of vertical nanowires self-arranged in lines with the length of several micrometers. The one-dimensional alignment of the wires proves that the Au-Si alloy islands arranged at the steps can be used as catalysts for nanowire formation. The SEM images also show that the wires have a fairly constant length and diameter. Figure 2 shows cross-sectional transmission electron microscopy (TEM) images and energy-dispersive X-ray spectroscopy (EDS) mappings of a GaP nanowire. There are no apparent defects passing through the nanowire/substrate interface, which is a promising feature for the integration of III-V semiconductor photonics into Si electronics.

Our approach to control the size and position of nanowires does not involve any "top-down" lithographic techniques; it is a pure "bottom-up" self-assembly method. Self-assembly has potential advantages of low cost, large scale, high quality, and so on, but there still remain lots of problems to be solved, especially in the controllability of the size and position of nanostructures. We hope that our approach will contribute to establishing self-assembled nano-device fabrication methods.

[1] H. Hibino and Y. Watanabe, Surf. Sci. **588** (2005) L233.
[2] K. Tateno, H. Hibino, H. Gotoh, and H. Nakano, Appl. Phys. Lett. **89** (2006) 033114.

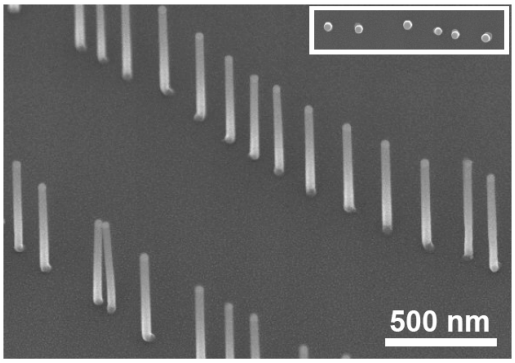

Fig. 1. An SEM image of GaP nanowires viewed from the direction inclined 38° from the surface normal. Inset: top view.

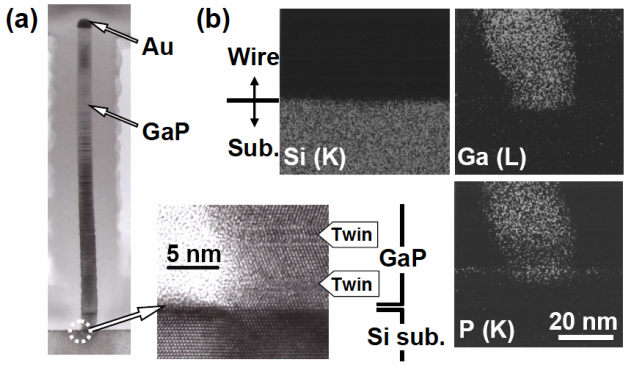

Fig. 2. A TEM image of a GaP nanowire. (b) EDS mapping images of Si, Ga, and P at the nanowire/substrate interface.

Microchannel Device Using Self-Spreading Lipid Bilayer as Molecule Carrier

Kazuaki Furukawa
Materials Science Laboratory

Self-spreading is a lipid wetting process at a solid-liquid interface, where a single supported lipid bilayer (SLB) is formed by a self-assembly process at the rim of a lipid spot adhering to a hydrophilic surface. We examined the self-spreading on the patterned surface and found that self-spreading occurs only on the hydrophilic surface of SiO_2. This led us to propose a new type of microchannel device, which we call "lipid-flow chip" [1].

The device structure and principle of the device operation are shown schematically in Fig. 1. The device is equipped with microchannel part of 10 μm wide and 400 μm long, and has a well on each side, which has been fabricated by conventional photolithography and lift-off process. A single self-spreading SLB grows only on hydrophilic surfaces after the SLB has been introduced into the pattern. When two SLBs collide in the middle of the channel, they form a unified SLB where molecular diffusion from one side to the other becomes dominant. SLBs are used only for transporting the molecules of interest. Thus an SLB is regarded as, for instance, a carrier gas for gas chromatography.

The device is beneficial for detecting an intermolecular interaction. As one example, we demonstrate the observation of fluorescence resonance energy transfer (FRET) between a donor (CC2) and an acceptor (FITC). As shown in Fig. 2, two lipid bilayers containing each dye-conjugated molecule was collided with each other in the microchannel. After the collision, they form a unified lipid bilayer, and the dyes are mixed with each other by lateral diffusion. The distribution of dye concentration is symmetrical to the point of the collision. A great reduction in donor fluorescence is, however, observed in a mixed area of donor and acceptor. This is because of the two relaxation processes, emission and FRET, exists in excited donor. The great reduction of donor emission is attributed to the effective FRET. Our device is also advantageous for quantitative analyses of FRET efficiency between a variety of dye pairs.

We plan to apply the technique to enzymes and proteins in order to study molecular interactions such biomolecules have.

[1] K. Furukawa, et al., Lab Chip **6** (2006) 1001.

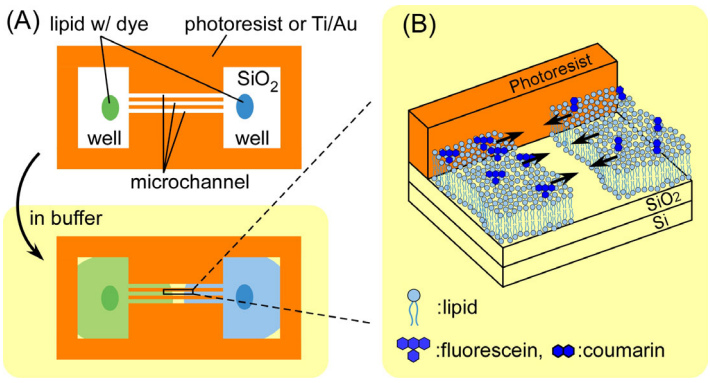

Fig. 1. Device structure and principle of the operation. L-α-PC extracted from egg yolk is used for the carrying medium of dye-conjugated lipid molecules.

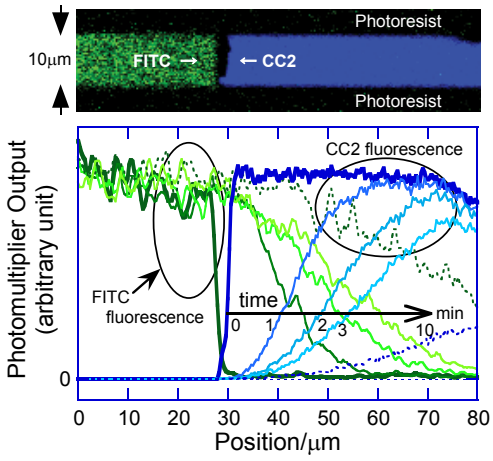

Fig. 2. Time-lapse observation of FRET. 5% of CC2- and FITC-conjugated lipid are mixed in L-α-PC.

Self-assembly of Vesicle Nanoarrays on Si: A Potential Route to High-density Functional Protein Arrays

Chandra S. Ramanujan[1], Koji Sumitomo[2], Maurits R. R. de Planque[1], Hiroki Hibino[2], Keiichi Torimitsu[2], and John F. Ryan[1]
[1]University of Oxford, [2]Materials Science Laboratory

DNA arrays have played a critical role in developing our understanding of genomics. However, whilst they can measure the expression levels of large numbers of genes simultaneously, they cannot be used to further characterize the protein products of such genes and their activity. An important objective of current research is to extend the use of array technology to both directly study the function of the proteins to aid drug discovery. Whereas DNA microarray technology is well-developed, the protein equivalent is still at the early stages of development. Protein microarrays have been recognized as a valuable tool since they require only a nanolitre-scale sample volume with a few picograms of the target protein or drug.

We show that 100 nm unilamellar thiol-tagged vesicles bind discretely and specifically to Au nanodots formed on a Si surface (See Fig.1). An array of such dots, consisting of 20 nm Au-Si three-dimensional islands, is formed by self-assembly on terraces of small-angle-miscut Si(111) after Au deposition [1]. Consequently, both the formation of the nano-pattern as well as the subsequent attachment of the vesicles are self-organized and occur without the need for any 'top-down' lithographic processes. This approach has the potential to provide the basis of a low-cost, high-density nanoarray for use in proteomics and drug discovery.

Today's DNA microarray technology has the potential of screening up to 10^5 ~10^6 probes in a 300 μl solution volume. In our nanodot arrays about 10^9 nanodots are covered by a 10 μl droplet [2]. The next steps towards producing a protein chip will include reconstituting proteins into the vesicles and determining a reliable way of labeling and reading the array, possibly using scanned probe techniques such as AFM or a combination of AFM and Scanning Near-field Optical Microscopy (SNOM). The AFM-SNOM has a resolution of about 100 nm. The gold-silicon combination provides an ideal substrate with a low background for fluorescence detection techniques. One way of producing a protein nanoarray would be to first scan and locate each nanodot, and then repeatedly expose to different protein-vesicle solutions and re-scan, until the chip is fully loaded. The deposition of a number of different protein-vesicles can be achieved by optimizing exposure time and vesicle density. The interaction of these mapped vesicle-proteins with fluorescent-labeled antibodies could be detected using the AFM-SNOM.

[1] H. Hibino and Y. Watanabe, Surf. Sci. **588** (2005) L233.
[2] C. S. Ramanujan, et al., App. Phys. Lett. **90** (2007) 033901.

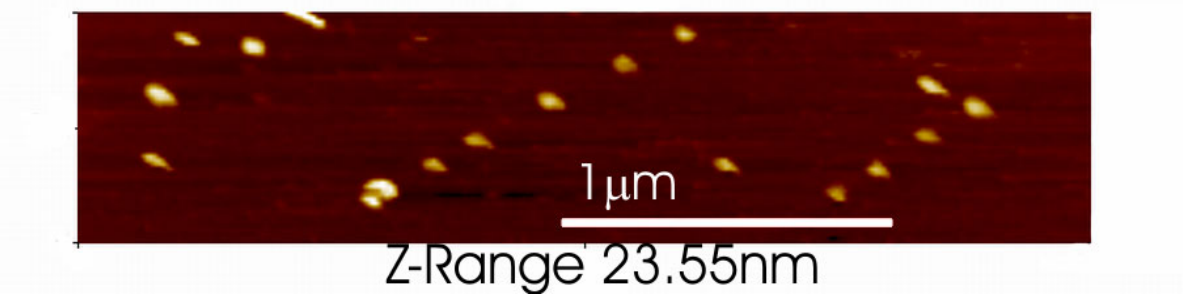

Fig. 1. AFM image of nanodot rows with vesicles that are modified to specifically attach to the gold nanodots formed by an earlier self-assembly process.

Ion Conducting Polymer Microelectrodes for Interfacing with Neural Networks

Tobias Nyberg, Akiyoshi Shimada, Nahoko Kasai, and Keiich Torimitsu
Materials Science Laboratory

We have examined the stimulation and recording properties of conjugated polymer microelectrode arrays as interfaces with neural networks of dissociated cortical neurons.

The polymer electrodes were electrochemically polymerized from a blend of poly (3,4-ethylenedioxythiophene)-poly (styrenesulfonate) (PEDOT-PSS) and ethylenedioxythiophene (EDOT) onto indium tin oxide (ITO) microelectrodes. Conducting polymers have been utilized to increase the surface roughness and improve the performance of planar electrodes [1].

The stimulation properties were investigated as a means of supplying a neural network with information. The impedance of the polymer electrodes (circles) was markedly lower than that of the ITO electrodes (squares) for low and medium frequencies and the phase of the polymer electrodes (solid line) was lower than that of the ITO electrodes (dashed line) for medium frequency as shown in Fig. 1. The peak current was proportional to the applied voltage pulses for polymer electrodes.

Dissociated cortical neurons from Wister rat embryos (embryonic day 18) were then plated on the electrodes and cultivated to form neural networks. Spontaneous activity was detected by both bare ITO and polymer electrode after 5 days in vitro and the bursting frequency increased as the networks matured. The stimulation efficiency at low voltages was evaluated and referenced to ITO electrodes. Polymer electrode stimulation evoked a much greater response from the network than stimulation from ITO electrodes as seen in Fig. 2. Polymer electrodes could be used at low stimulating potentials for the efficient stimulation of neuronal tissue for more than one month and interfacing could be maintained for several months. These results show that conducting polymer electrodes have the biocompatibility needed microelectrodes for interfacing with neural networks.

[1] T. Nyberg, et al., J. Neurosci. Methods. **160** (2007) 16.

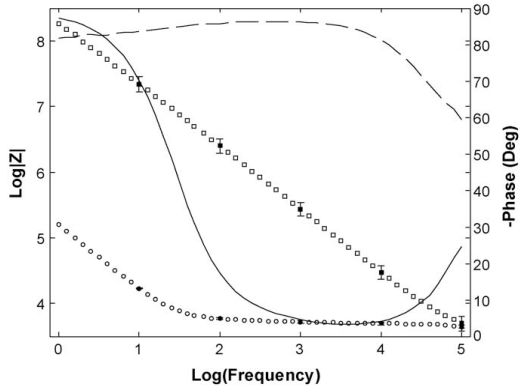

Fig. 1. Bode plot of polymer and ITO electrodes.

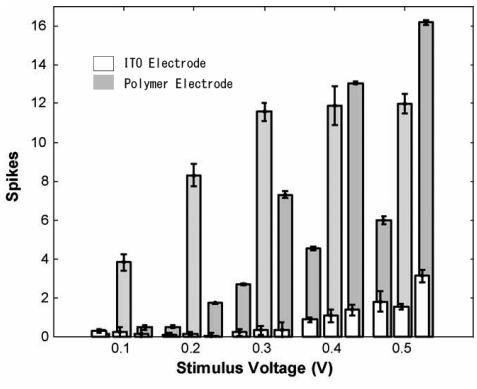

Fig. 2. Evoked response for polymer and ITO stimulation.

Ion Sensing Assisted by Assembly of Gold Nanorods

Hiroshi Nakashima and Kazuaki Furukawa
Materials Science Laboratory

Rod-like gold nanoparticles (gold nanorods: NRs) show their shape and size-dependent optical properties whose origin is localized surface plasmon resonance (LSPR). The rod-shaped geometry has an inherently high sensitivity to the local dielectric environment including the adsorbates and the interparticle spacing of the NRs. Therefore, gold NRs have promising applications as analytical probes in biotechnological systems.

Herein, we report the selective ion sensing of physiologically important cations such as Na^+ and K^+ using the LSPR absorption of gold NRs with thiol-modified crown ethers in response to dispersed and aggregated gold NRs. The crown ethers attached themselves covalently to the gold NR surface due to the high affinity of the thiol group to gold [1].

Figure.1 shows the absorption spectra of the gold NRs (length: 40 nm, diameter: 10 nm) with 15-crown-5-SH on the addition of NaCl or KCl solution. The gold NRs exhibited two plasmon absorption maxima around 680-700 and 520 nm, corresponding to a longitudinal mode along the long axis and a transverse mode perpendicular to the long axis, respectively. When we increased the amount of added KCl solution, the longitudinal absorption intensity of the NRs gradually decreased and the peak was blue-shifted. The spectral change was caused by the formation of NR aggregates. The recognition of K^+ is proposed via a sandwich complex of 2:1 between 15-crown-5 moiety and K^+ (Fig. 2). This triggered the coupling of the plasmon absorbance as a result of the NRs proximity to each other. In the presence of Na^+, the absorption spectra profiles of gold NRs with 15-crown-5-SH remained largely unchanged. The results originated from the fact that Na^+ was recognized by simple 1:1 host-guest interactions that correlated with the close fit of the cation to the crown cavity. Consequently, the dispersed or aggregated states of the gold NR complex, which is dominated by the ion sensing mechanism, result in further spectral changes.

The LSPR properties of gold NRs can be continuously tuned by adjusting their aspect ratio from the ultraviolet to the infrared region, including the near-infrared region where tissue transmissivity is at its highest. The functionalized gold NRs with various biomolecules will provide nano detection platforms such as those used for diagnostic applications and biological imaging, and function as a colorimetric reporter *via* the highly sensitive LSPR properties.

[1] H. Nakashima, et al., Chem. Commun. (2007) 1080.

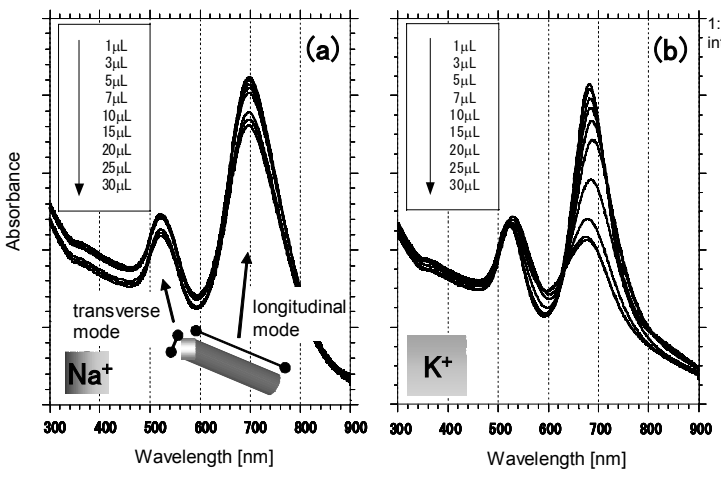

Fig. 1. Absorption spectrum changes of gold NRs on addition of (a) Na^+ and (b) K^+.

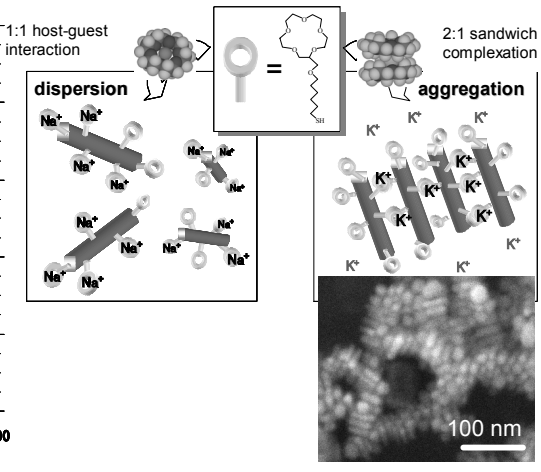

Fig. 2. Mechanism of ion recognition and SEM image of assembled gold NRs.

Terahertz Spectroscopy of Biomolecules in Nanospace

Katsuhiro Ajito[1], Yuko Ueno[1,2], Rakchanok Rungsawang[1], and Isao Tomita[1,3]
[1]Materials Science Laboratory,
[2]NTT Microsystem Integration Laboratories, [3]NTT Photonics Laboratories

Terahertz (THz) wave region around 0.3 – 10 terahertz has attracted much attention in spectroscopy since it can reveal weak chemical bonds in molecules. We have recently shown that THz time-domain spectroscopy (THz-TDS) using THz wave pulses exhibits sufficient sensitivity to molecules to be used as a tool in analytical chemistry [1, 2].

Figure 1 shows angle-dependent THz-TD absorption spectra of cystein single crystal measured by using linearly polarized THz wave. An *ab initio* frequency calculation of a single amino acid molecule was used to predict the intramolecular vibrational modes. These provide high absorption when molecules are probed with a THz electric field whose polarization is parallel to the oscillating dipole directions [3].

Figure 2 shows THz-TD absorption spectra of two steric isomers, namely fumaric acid and maleic acid molecules in nanosized pores of a mesoporus silicate and their crystals in polyethylene pellets. The intermolecular modes observed with fumaric acid crystals are inactivated by incorporating the molecules in the nano-sized pores due to the separation of the molecules, whereas the intramolecular modes of maleic acid for the crystal and the incorporated samples are similar [4]. Incorporating target molecules in nano-sized spaces is effective in reducing the concentration of the intermolecular hydrogen bonds of the sample, and it is possible to distinguish intramolecular hydrogen-bonding vibrational modes from intermolecular hydrogen-bonding vibrational modes.

We believe that THz spectroscopy will open a new filed in biological analysis in nanospace.

[1] K. Ajito, R. Rungsawang, I. Tomita, and Y. Ueno, Electrochemistry **74** (2006) 506.
[2] Y. Ueno, R. Rungsawang, I. Tomita, and K. Ajito, Anal. Chem. **78** (2006) 5424.
[3] R. Rungsawang, Y. Ueno, I. Tomita, and K. Ajito, J. Phys. Chem. B, **110** (2006) 21259 .
[4] Y. Ueno, R. Rungsawang, I. Tomita, and K. Ajito, Chem. Lett. **35** (2006) 1128.

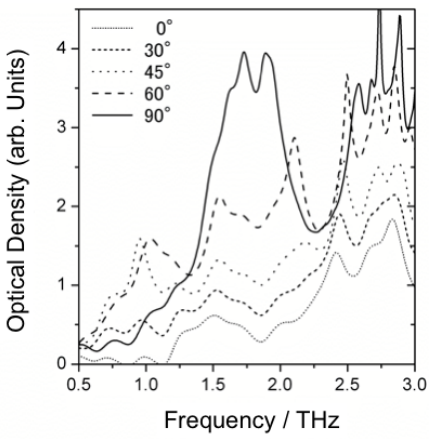

Fig. 1. Angle-dependent THz-TD absorption spectra of cystein single crystal at room temperature. 0° is defined when the *c*-axis of the crystal is parallel to the polarization of the THz field.

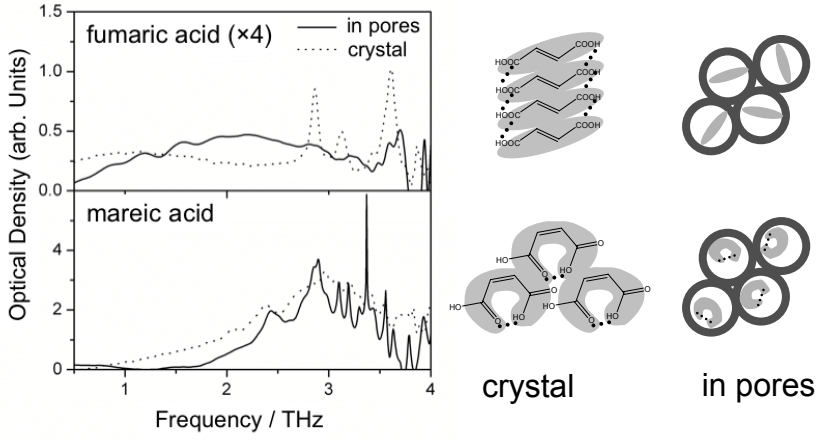

Fig. 2. THz-TD absorption spectra of fumaric acid and mareic acid molecules (upper and lower) in nanosized pores of a mesoporus silicate (solid lines) and their crystals in polyethylene pellets (dotted lines) at 77K.

Gain-cell Dynamic Random-access Memory with Long Data Retention

Katsuhiko Nishiguchi, Yukinori Ono, and Akira Fujiwara
Physical Science Laboratory

As the information technology market continues to expand in various fields, the performance of data information processing circuits has been improved with an increase in memory capacity. The capacity of dynamic random-access memory (DRAM), which stores information data as charges in a memory node (MN), has been increased by shrinking the DRAM cell. However, further reduction in a MN capacitance would cause the stored signal to be buried in noise. Therefore, cell miniaturization and a conservation of the MN capacitance should be achieved simultaneously. This requires complicated structures and new materials, which leads to higher difficulties and costs in their fabrications.

One class of memory device that could allow further shrinking of the MN is a gain-cell DRAM, in which a small signal originating from electrons stored in the MN is amplified by a nearby transistor. However, good scalability of the MN in the gain-cell DRAM raises another problem: a smaller MN means fewer electrons in the MN, which leads to shorter retention time. The dominant origin of this short retention is a current leakage originating from a p-n junction formed in the MN. A consequence of this problem is that the data-refresh process, i.e., periodic data read-out and storage, would have to be performed more frequently than in ordinary DRAMs, which would increase power consumption.

We thus fabricated a log-data-retention gain-cell DRAM without p-n junction. The device is composed of two transistors, FET1 and FET2, which transfer and detect electrons, respectively. Both were fabricated on an undoped silicon-on-insulator (SOI) wafer (Fig. 1)[1]. The upper gate (UG) is used to induce an inversion layer in the undoped FET1 channel. When the lower gate (LG) turns FET1 off, an energy barrier under the LG electrically forms the MN at the tip of the wire channel of FET1. By opening and closing FET1, the data '0' and '1' are respectively represented by the presence and absence of electrons in the MN, which are introduced from the electron reservoir (ER). Then, the stored data, i.e. electrons, are read out as the change in current flowing through FET2, which is capacitively coupled to the MN.

Figure 2 shows that the fabricated device provides extremely long data retention (~10^4 s) even at 85 °C. This is because the p-n junction formed at the boundary of the MN and FET1 in conventional DRAMs is replaced with the inversion layer formed by the UG, as shown in the insets of Fig. 2. Additionally, fast data storage (~10 ns) and dynamic random access comparable to those of conventional DRAMs were also confirmed.

The demonstrated long data retention reduces the data-refresh cycles, thereby leading to low power consumption. The fabrication process is highly compatible with MOSFET circuits and is therefore promising for building gain-cell DRAMs embedded into logic circuits.

[1] K. Nishiguchi, et al., IEEE Electron Device Lett. **28** (2007) 48.

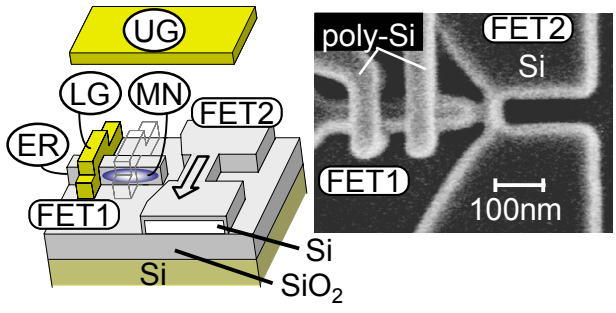

Fig. 1. Structures of gain-cell DRAM.

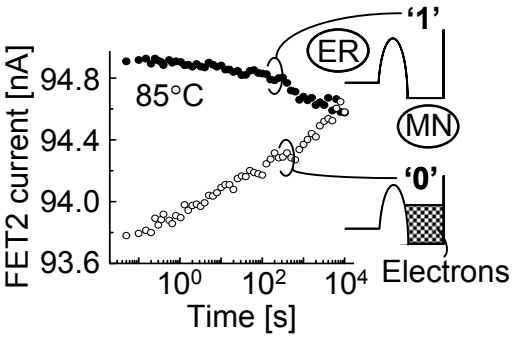

Fig. 2. Data-retention characteristics.

Detection of Single Boron Acceptor in Silicon Nano-transostor

Yukinori Ono, Katsuhiko Nishiguchi, and Akira Fujiwara
Physical Science Laboratory

Highly scaled metal-oxide-semiconductor field-effect transistors suffer serious problems from the fluctuation of the dopant-atom number, but in turn, offer a new concept of a device in which the charge transport is regulated by means of only a few dopant atoms. It is therefore important to obtain a deeper understanding of the effect of dopants on charge transport in transistors [1-3] and also to establish a technology for detecting and controlling the dopant charges. Here, we report the detection of a single boron acceptor in a small transistor as a first step towards the realization of *single-dopant technology* [4].

Nano transistors whose gate length and width are both 40 nm were fabricated on a silicon-on-insulator substrate. The transistors comprise the channel lightly doped with boron, p-type source/drain, and electrically formed leads inserted between the channel and the source/drain. The insertion of the leads prevents the dopant diffusion from the source/drain and enables us to investigate the conductance of the channel containing only a few dopant atoms. The conductance was measured at 26 or 6 K as a function of the gate voltage using the substrate voltage (V_{BG}) as a parameter. Figure 1 shows examples of the conductance characteristics for transistors with the doping density of 2×10^{16} cm^{-3}, corresponding to the mean boron number in the channel of around one. The conductance modulation, indicated by the arrows, was observed in such lightly doped transistors but not in undoped ones. Figure 2 shows the differential conductance as functions of the gate and drain voltages, which demonstrates that the conductance modulation in Fig. 1 is due to the capture and emission of a single hole by and from a single boron acceptor.

The conductance level of the modulation peak was strongly dependent upon V_{BG} and the dependence was different from one transistor to another (Fig. 1), which is because of the random doping of boron atoms. This suggests that the V_{BG} dependence conveys the information about the location (depth) of the boron and thus could lead to a way to count the dopant-atom number and measure the location of individual dopant atoms in a transistor.

[1] Y. Ono, et al., Jpn. J. Appl. Phys. **44** (2005) 2588.
[2] Y. Ono, et al., Phys. Rev. B**74** (2006) 235317.
[3] J.-F. Morizur, et al., Phys. Rev. Lett. **98** (2007) 166601.
[4] Y. Ono, et al., Appl. Phys. Lett. **90** (2007) 102106.

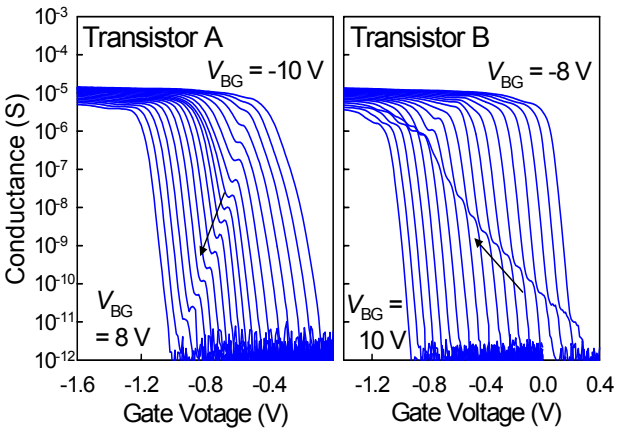

Fig. 1. Conductance at 26 K of transistors whose mean boron number in the channel is around one.

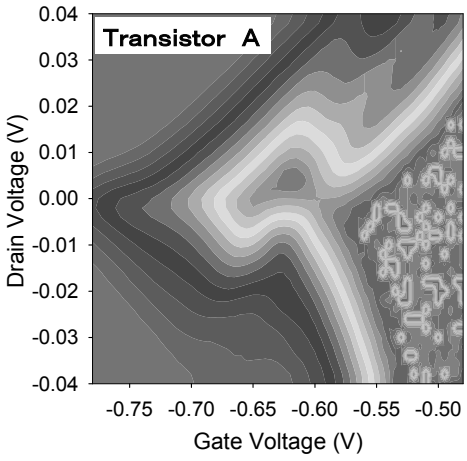

Fig. 2. Differential conductance measured at 6 K.

Electron Phase Sensing in a High Q Mechanical Resonator

Imran Mahboob and Hiroshi Yamaguchi
Physical Science Laboratory

Electromechanical systems are novel devices incorporating a high Q mechanical oscillator within an electrical architecture. Due to their low energy dissipation characteristics, these devices offer unprecedented sensitivity for the detection of miniscule forces arising from for example magnetic moments, electron and nuclear spins. Furthermore, the purity of the mechanical mode enables fundamental energy dissipation processes to be studied for example electron-electron and electron-phonon interactions in quantum electron transport in low dimensional systems.

In this study, modulations in the phase of the electron wave function were used to detect the miniscule displacements of the mechanical element [1]. A quasi-1D diffusive electron system in an InAs quantum well was incorporated onto an AlGaSb nano-mechanical suspended beam and is shown in Fig.1(a). Additionally, a Au wire was also placed on the suspended beam to enable the mechanical resonance to be actuated via the magnetomotive method where an alternating current was passed in the Au channel in the presence of a magnetic field. An out of plane beam resonance frequency, f_0 = 10.268 MHz and quality factor, Q = 12500 was measured at 20 mK and is shown in Fig.1(b).

The beam oscillation was then detected by measuring the resistance change in the quasi-1D electron system as a function of beam vibration frequency and magnetic field. The resistance change at the beam resonance frequency (magnetopiezoresistance [MPR]) was strongly peaked. By varying the magnetic field, this resistance change at resonance could be modulated. The MPR at mechanical resonance showed reproducible highly periodic resistance oscillations which arise via strain induced electron phase modulation and is shown in Fig.1(c). The Fourier transform of the MPR [shown in Fig.1(d)] indicates that mechanical activation of the beam affects only a few electron trajectories and the electron interference in only a single electron loop gives rise to the resistance oscillations observed in the MPR.

[1] I. Mahboob, et al., Appl. Phys. Lett. **89** (2006) 192106.

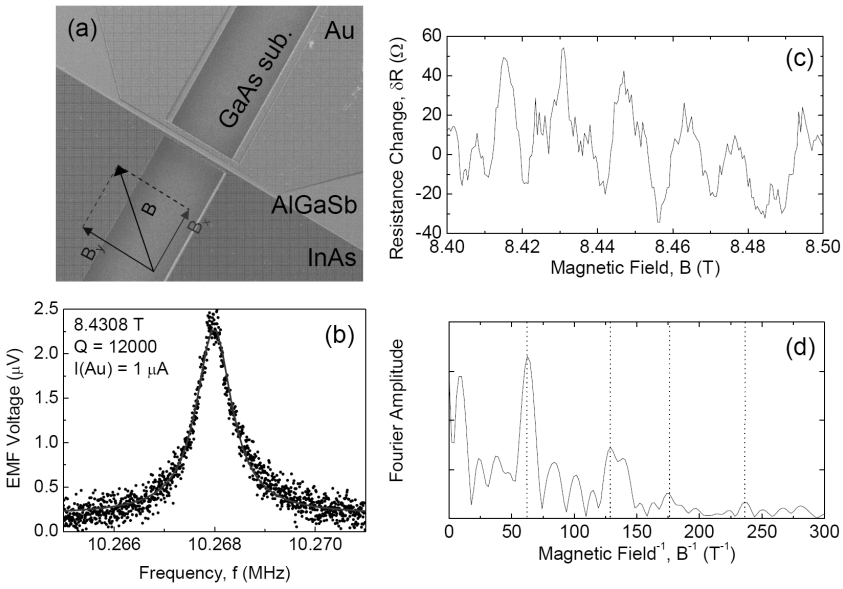

Fig. 1. An SEM image of the device (8 μm long and 1.5 μm wide) (a). The beam resonance measured by the magnetomotive method (b). The MPR, measured at mechanical resonance in the quasi-1D InAs system (c). The Fourier transform of the MPR (d).

Block Copolymer Lithography toward 16-nm-technology Nodes

Toru Yamaguchi and Hiroshi Yamaguchi
Physical Science Laboratory

Block copolymer lithography (BCL) has attracted considerable attention as a combined top-down/bottom-up approach to nanopatterning. It involves the use of microphase-separated nanometer-sized domains of block copolymers as lithography templates. In recent times, the significance of BCL in the field of lithography is particularly increased due to the fact that top-down lithography will soon be reaching its limit in the 22-nm regime, necessitating the development of innovative technologies. BCL has great potential for exceeding the resolution limit of the state-of-art top-down lithography because its resolution is determined solely by the molecular size of the block copolymer. The most important challenge in BCL is the achievement of a strict control on the alignment of various microphase-separated domains. Among these domains, vertical lamellar domains composed of alternating stacked layers of two dissimilar polymer chain blocks A and B (Fig. 1) have critical advantages as lithography templates for nanodevice fabrication on account of their line shape, high aspect ratio, and wide flexibility in pattern configuration. However, the difficulty encountered in the formation of vertical lamellae was that the lamellar interface should be aligned in two directions, perpendicular to the substrate surface and parallel to the lithographically created features.

Here, we report our novel method of aligning lamellar domains by means of graphoepitaxy using a resist pattern as an alignment guide [1]. Graphoepitaxy is a technique that uses the surface topography of the substrate to direct the epitaxial growth of the block copolymer film. The key to its success is the combination of the neutralization of a bottom surface and the introduction of a hydrophilic guiding pattern; this makes it possible to independently control the surface affinity of the substrate surface and the sidewall surface of the guiding pattern, which leads to the vertical orientation and lateral alignment of lamellar domains, respectively (Fig. 1). We have successfully demonstrated that the lateral alignment of the lamellar structure of a symmetric poly(styrene-*b*-methyl methacrylate) is achieved in confined spaces of about $3L_a$ (L_a: laterally aligned lamellar period, L_a ~ 32 nm) between hydrogen silsesquioxane (HSQ) resist patterns on a neutral surface (Fig. 2). It is important to consider that a lamellar structure with a period shorter than the pitch of the guide pattern could be formed by this method. We believe that the combination of the artificial layout of the guide patterns and the best polymer materials could lead to a new type of high-resolution lithographic technology in the 16-nm ($1/2\ L_a$) regime.

[1] T. Yamaguchi and H. Yamaguchi, J. Photopolym. Sci. Technol. **19** (2006) 385.

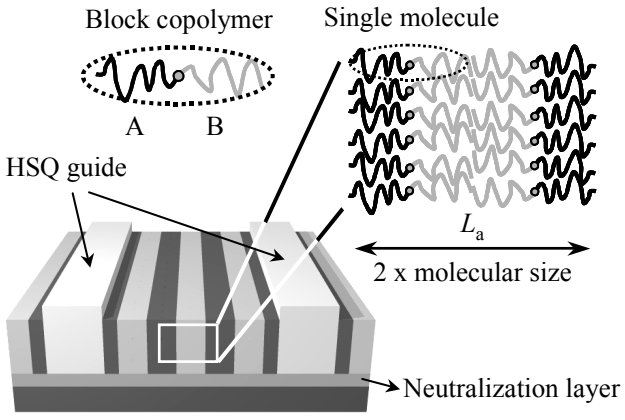

Fig. 1 Lateral alignment of lamellar domains.

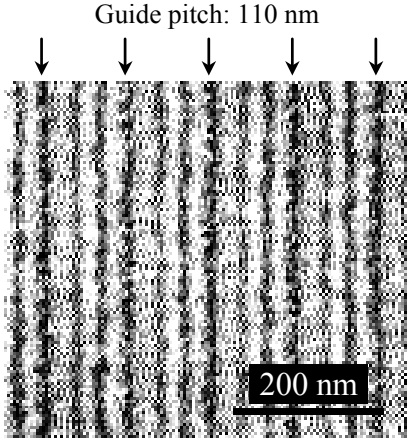

Fig. 2 AFM phase image of aligned domains.

Single-electron Counting Device

Toshimasa Fujisawa
Physical Science Laboratory

Single-electron counting device (see a frontispiece) is promising for detecting individual electron flow and analyzing an electrical current with various statistical analyses. Here, we present some experiments as a single-electron ammeter for detecting an extremely faint current and as a physical tool to investigate electron correlation in a transport [1].

We have developed a single-electron counting device, which measures the location of an electron in two quantum dots by using a point contact electrometer (see the frontispiece). For example, an average current can be obtained by counting the number of net electron flow in a given period. We have demonstrated such current measurement on a single-electron transistor as shown in Fig. (a). The obtained current shows Coulomb blockade oscillations as shown in Fig. (b), where noise level of about 3 atto-ampere is three or four orders of magnitudes smaller than that in a conventional ammeter.

In addition to the average current, various statistical analyses are also demonstrated. Figure (c) shows a histogram of the interval between two consecutive forward electron tunneling events (called forward recurrence time), where the reduction of the occurrence with zero interval suggests anti-bunching correlation. This appears from Coulomb interaction in the single-electron transport through the counting device. Moreover, Fig. (d) represents a histogram of the current measured in a short period T_{avr} (counting statistics), where higher order noise of the current are extracted to characterize the distribution of the current. We believe that various correlated transport can be examined with this technique.

[1] T. Fujisawa, et al., Science **312** (2006) 1634.

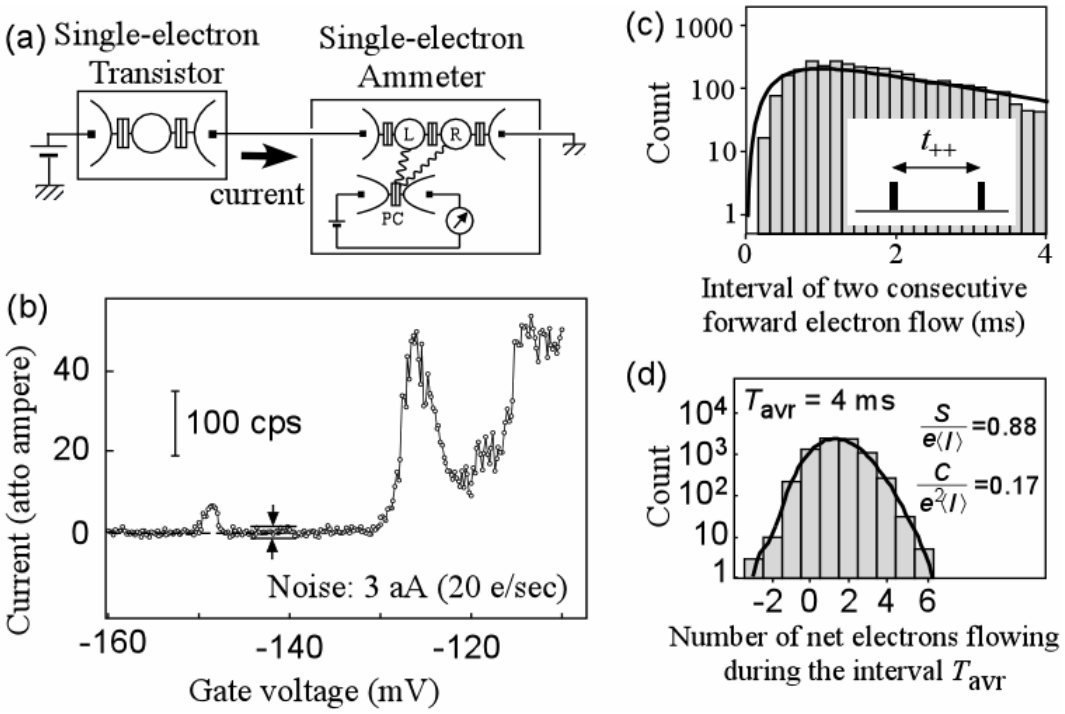

Fig. Experiments on single-electron counting. (a) A circuit diagram for measuring a current from a single-electron transistor. (b) Coulomb blockade oscillations of the device. (c) Anti-bunching correlation in the transport through the device. (d) Counting statistics of the current showing the second (S) and third (C) order noise.

Density-of-states Imaging in Semiconductor Heterostructures

Kyoichi Suzuki[1], Kiyoshi Kanisawa[1], Simon Perraud[1,2], Camille Janer[1,3],
Kei Takashina[1], Toshimasa Fujisawa[1], and Yoshiro Hirayama[1,4]
[1]Physical Science Laboratory, [2]CNRS, [3]ESPCI, [4]Tohoku University

As semiconductor devices develop and become highly integrated with ultra fine processes, quantum mechanical effects in the devices dominate their characteristics. Local analysis of the wavefunctions becomes important for realizing precise device performance. In addition, new physical phenomena emerging from their nano-scale dimensions are expected. The scanning tunneling spectroscopy (STS) method, which measures the tunneling current characteristics using a scanning tunneling microscope (STM), allows us to investigate the electron density of states (DOS) with nanometer resolution as a function of the energy, corresponding to the squared wavefunctions. By scanning the probe, the spatial distribution of the DOS can be obtained.

By performing STS on cleaved semiconductor heterostructure surfaces (Fig. 1), we have succeeded in imaging quantized subbands formed in a quantum well (Fig. 2) [1], interference of electron waves at an heterointerface (Fig.3) [2], and wavefunction coupling in a double quantum well [3]. This method can be easily applied to more complicated heterostructures allowing spatial wavefunction analysis in real devices.

[1] K. Suzuki, et al., Phys. Rev. Lett. **98** (2007) 136802.
[2] K. Suzuki, et al., Jpn. J. Appl. Phys. **46** (2007) 2618.
[3] K. Suzuki, et al., J. Cryst. Growth **301-302** (2007) 97.

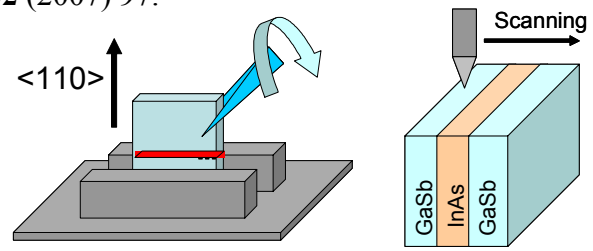

Fig. 1. Cleaving is performed under ultra-high vacuum (UHV) (<2x10^{-10}Torr) to obtain a clean flat surface. Then, the sample is loaded into the STM setup cooled down to 4.8 K without breaking UHV.

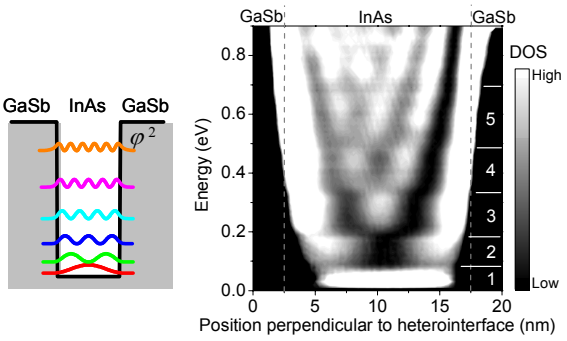

Fig. 2. DOS in an InAs/GaSb single quantum well. Spatial standing wave patterns corresponding to the confined subbands were observed.

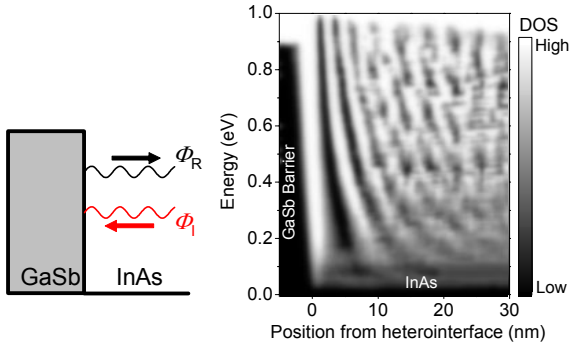

Fig. 3. DOS around an InAs/GaSb single heterointerface. Interference patterns due to the electrons incident on/reflected from the GaSb potential barrier were observed.

Quantum Transport in Silicon-On-Insulator Structures

Kei Takashina, Yukinori Ono, Akira Fujiwara, Yoshiro Hirayama*, and Toshimasa Fujisawa
Physical Science Laboratory

Besides being of immense technological importance, electrons in silicon offer a number of unique possibilities for exploring new physical conditions and new phenomena. One of these arises due to their bulk dispersion relation where there are six, energetically degenerate conduction band valleys. In Si(100)-MOSFETs where electrons are two-dimensionally confined, this six-fold degeneracy is lifted, due to anisotropic effective mass, to leave only two low lying valleys available for occupation. 2-D electrons in such structures consequently have freedom as to how they occupy these degenerate valleys giving them a valley degree of freedom on top of in-plane motion and spin.

In the present study, we have been able to show that valley-splitting, which lifts this remaining two-fold valley degeneracy can be enlarged and controlled over an unprecedented extent using SOI (Silicon-On-Insulator) MOSFETs [1] and that its effects can be observed clearly by direct transport measurements even without magnetic field (Figures) [2]. The results demonstrate considerable potential for exploring valley-related phenomena and new device possibilities.

[1] K. Takashina, A. Fujiwara, S. Horiguchi, Y. Takahashi, and Y. Hirayama, Phys. Rev. B **69** (2004) 161304(R).
[2] K. Takashina, Y. Ono, A. Fujiwara, Y. Takahashi, and Y. Hirayama, Phys. Rev. Lett. **96** (2006) 236801.

*Present address: Tohoku University

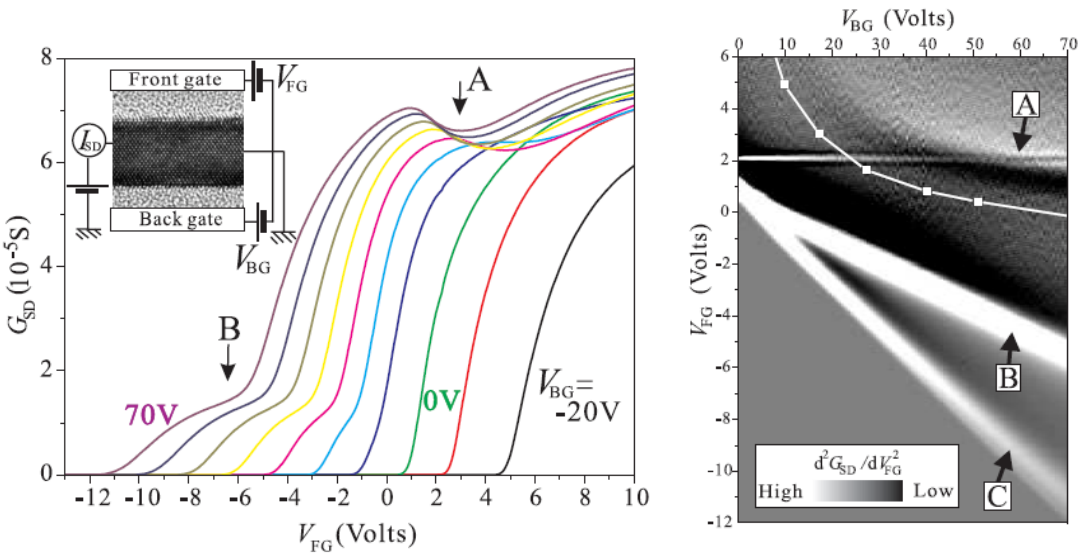

Fig. Two-terminal conductance at 4.2K as a function of front-gate voltage V_{FG} at various values of back-gate voltage V_{BG}. The inset shows the experimental setup. A and B mark features associated with second-confinement-subband occupation and valley splitting respectively. Right: 2nd derivative of the data showing the evolution of the features. The white squares joined by lines mark self-consistently calculated positions of the onset of second-confinement-subband occupation using nominal parameters of the device. (The feature marked C is due to the onset of conduction.)

Decoherence of a Superconducting Flux Qubit

Kosuke Kakuyanagi, Shiro Saito, Hayato Nakano, and Kouichi Semba
Physical Science Laboratory

In order to carry out quantum operations using qubits, we need to maintain quantum coherence throughout all the quantum gate operations. However, coherence decreases over time because of the interaction between qubits and their environment. This phenomenon is called decoherence, and we must clarify its origins if we are to extend the coherence time.

The superconducting flux qubit (Fig. 1) is a promising solid-based qubit that offers the advantage of scalability. We attempt to measure the magnetic field dependence of the phase relaxation time (T_2) and energy relaxation time (T_1) in order to clarify the decoherence of a superconducting flux qubit [1]. Relaxation is generally caused by the energy fluctuation that is generated from the interaction between qubits and their environment. Therefore, we can obtain information about the contribution of magnetic fluctuations to decoherence from field dependence measurements of the relaxations.

Figure. 2 shows measurement results for the magnetic field dependence of T_1 and T_2 near the degeneracy point ($\Delta\Phi_{qb} = 0$). The magnetic field is plotted with flux quantum units (Φ_0). The T_2 values increase as the external magnetic field approaches the degeneracy point. At the degeneracy point, the T_2 value reaches 250 ns. In contrast, the T_1 values are uniform ($T_1 \sim 140$ ns).

In general, T_2 includes pure dephasing (Γ_Φ) and T_1 component contributions. The relationship between T_1 and T_2 is described as $1/T_2 = \Gamma_\Phi + 1/(2T_1)$. From the observed T_1 and T_2 values, the coherence time of a superconducting flux qubit at the degeneracy point is mainly suppressed by energy relaxation. Moreover, we can explain the behavior of the magnetic field dependence of pure dephasing in terms of the contribution of $1/f$ type frequency distributed magnetic fluctuations.

Energy relaxation is generated from high frequency fluctuations, whose frequency is the same as the qubit energy. These results suggest that the coherence time of a superconducting flux qubit improves when we suppress the high frequency noise. Next, we will attempt to improve the coherence time of the superconducting flux qubit.

[1] K. Kakuyanagi, et al., Phys. Rev. Lett. **98** (2007) 047004.

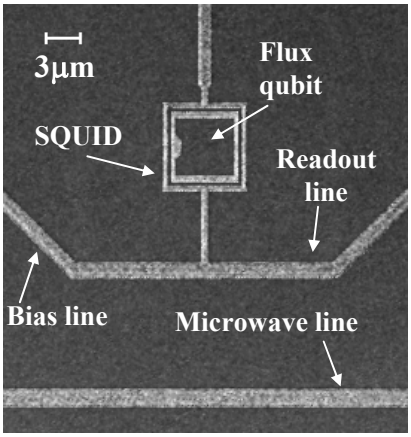

Fig. 1. Sample image of flux qubit.

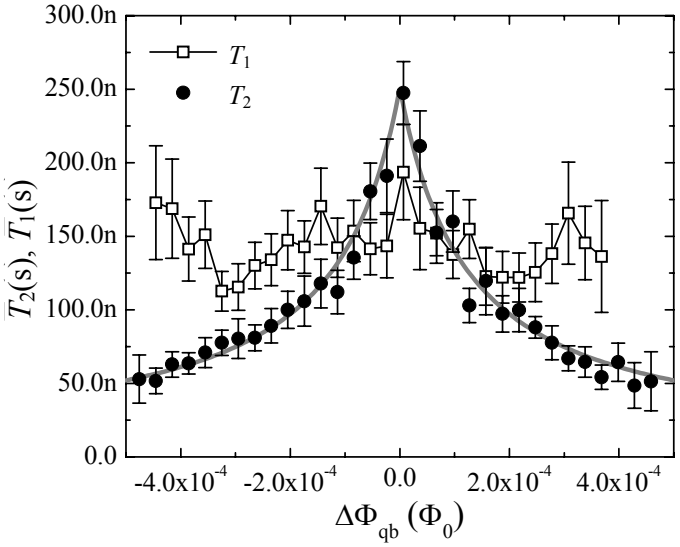

Fig. 2. Field dependence of T_1 and T_2.

Aharonov-Casher Effect by Spin-orbit Interaction

Tobias Bergsten[1,2], Toshiyuki Kobayashi[1,2], Yoshiaki Sekine[1,2], and Junsaku Nitta[1,2,3]
[1]Physical Science Laboratory, [2]CREST-JST, [3]Tohoku University

The aim of spintronics is to manipulate spin of electrons in electronic circuits. This will make it possible to design new kinds of electronic devices, e.g. the spin-FET proposed by Datta and Das [1]. The common way to manipulate spin is by using magnetic field, because the spin is related to magnetic properties. However, it is also possible to use an electric field to influence the spin, utilizing spin-orbit interaction (SOI). The strength of the SOI in a semiconductor heterostructure can be engineered by careful design of the conductance and valence bands, and it can also be controlled by an electrostatic gate on top of the device [2]. In the current study, we have controlled the interference of the electron waves due to spin precession by gate voltage [3]. This is a demonstration of the Aharonov-Casher (AC) effect, an interference of particles with magnetic moment interacting with an electric field.

The device used in this study was fabricated using InAlAs/InGaAs/InP quantum well, where the SOI strength is tunable by gate voltage by more than 3 peVm. To observe the interference of electron waves traveling along a limited path, a ring array was etched out as shown in Fig. 1. The gate electrode is deposited on top of the rings using 50 nm-thick SiO_2 as a gate insulator.

The relative phase difference of partial electron waves, which propagate clockwise and counterclockwise in a ring structure, was controlled by the gate voltage (AC effect) as well as the magnetic field (Aharonov-Bohm and Al'tshuler-Aronov-Spivak effect) and measured as a resistance oscillation (Fig. 2). Since the electron is a fermion particle (spin is 1/2), the spin precession of one turn (2π) changes the quantum phase for π. Therefore, the resistance oscillation period with respect to the gate voltage corresponds to the relative spin precession angle of 4π between the two partial waves of an electron traveling opposite directions and coming back to the original position. This shows that we have precise control of the spin precession angle for over 12π. This spin control is essential for the spin-FET and it may also prove important for future quantum computing devices based on spin qubits.

[1] S. Datta and B. Das, Appl. Phys. Lett. **56** (1990) 665.
[2] J. Nitta, T. Akazaki, H. Takayanagi, and T. Enoki, Phys. Rev. Lett. **76** (1997) 1335.
[3] T. Bergsten, T. Kobayashi, Y. Sekine, and J. Nitta, Phys. Rev. Lett. **97** (2006) 196803.

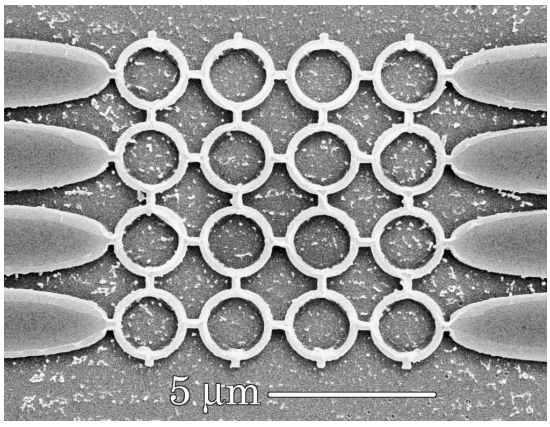

Fig. 1. SEM image of a ring array etched out of an InAlAs/InGaAs/InP heterostructure.

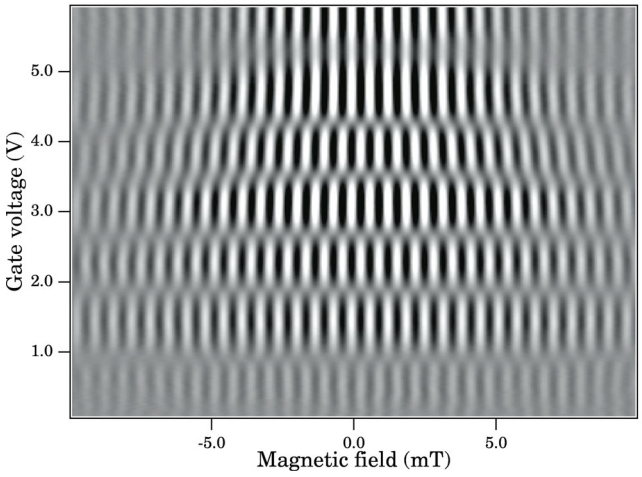

Fig. 2. The resistance oscillation by AC effect (vertical direction) and AAS effect (horizontal direction).

Detection of Domain Wall in a Permalloy Wire Using a Semiconductor and Ferromagnetic Hybrid Structure

Yoshiaki Sekine[1], Tatsushi Akazaki[1], and Junsaku Nitta[2,3]
[1]Physical Science Laboratory, [2]Tohoku University, [3]CREST-JST

Using the local Hall effect (LHE), we have succeeded in detecting a magnetic domain wall (DW) trapped in a permalloy, NiFe, wire and in clearly distinguishing whether the DW structure is a tail-to-tail or a head-to-head DW [1].

In the field of spintronics, devices utilizing DWs were proposed and many methods were applied to detect DWs. Among them, the LHE method using a semiconductor and ferromagnetic hybrid structure has the advantage of large signal enough to investigate the DW dynamics. An InGaAs two-dimensional electron gas (2DEG) that is 5 nm below the surface was used for a Hall sensor that detects the stray field from the NiFe wire. A 60-nm-thick and 300-nm-wide NiFe wire consisting of a notch at the center, a taper end and a right-angle end was deposited on the surface. These wire structures make it possible to trap a tail-to-tail or a head-to-head DW at the notch with changing the direction of the magnetic field, B. Three Hall crosses were fabricated just below both ends and the center of the wire. Figures 1(a) and (b) show a scanning electron microscopy (SEM) image and a cross-sectional view of the sample, respectively. A tail-to-tail DW and a head-to-head DW are sketched in Fig. 1(c) and (d). With sweeping B parallel both to the wire and the 2DEG, the DW nucleates at the right-angle end, then the DW displaces to and pins at the notch. With changing B furthermore, the DW depins from the notch, then the DW moves to and annihilates at the right-angle end. The B-dependence of the Hall resistivity, ρ_{yx}, on three Hall crosses is shown in Fig. 2. Here, $\rho_{yx}1$, 2, 3 are defined as ρ_{yx} on the right-angle end, notch, and taper end, respectively. With increasing B, $\rho_{yx}1$ shows the sharp drop at 22 mT, which corresponds to the DW nucleation at the right-angle end. At 26 mT, rapid increase of $\rho_{yx}3$ represents the DW annihilation at the taper end. Between 22 and 26 mT, $\rho_{yx}2$ shows the peak, which corresponds to the pinned tail-to-tail DW. With decreasing B, the sharp changes in $\rho_{yx}1$ and 3 represent the DW nucleation and annhilation. Between -22 and -26 mT, the dip of $\rho_{yx}2$ corresponds to the pinned head-to-head DW. Note that the DW nucleates at the right-angle end with sweeping B. The LHE method can make the distinction between the tail-to-tail and head-to-head DWs. These results indicate the LHE method is attractive for investigating the DW movement that is a key to DW devices.

[1] Y. Sekine, et al., AIP Conference Proceedings **893** (2007) 1291.

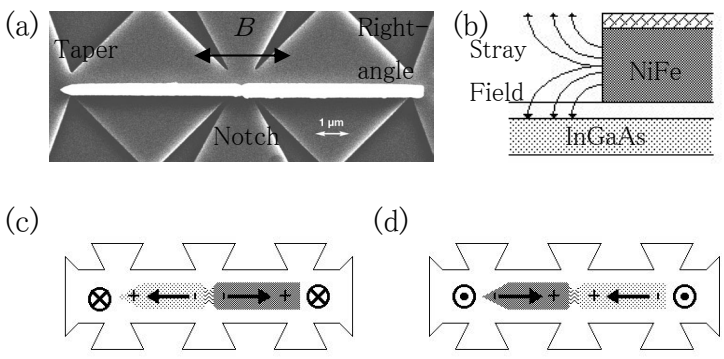

Fig. 1. (a) The SEM image of the sample. (b) The cross-sectional view of the sample. The schematic view of the (c) tail-to-tail and (d) head-to-head DWs.

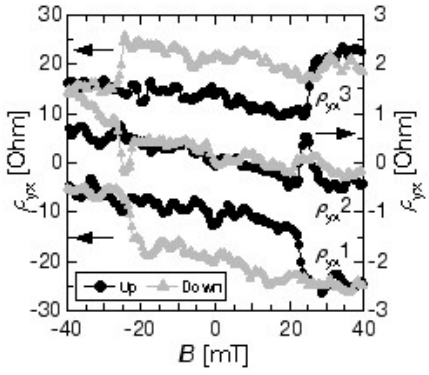

Fig. 2. The Hall resistivity, ρ_{yx}, vs the magnetic field, B. The peak and dip in $\rho_{yx}2$ correspond to the trapped tail-to-tail and head-to-head DWs.

Controllable Coupling between Flux Qubit and Nanomechanical Resonator by Magnetic Field

Y.D Wang, Hajime Okamoto, Hiroshi Yamaguchi, and Kouichi Semba
Physical Science Laboratory

Flux qubit, also known as persistent current qubit, is micro-meter sized superconducting loop interrupted by several (usually three) Josephson junctions. Flux qubit is one of the most promising candidates for physical realizations of quantum information processing. On the other hand, nanoelectromechanical systems (NEMS), whose scale is smaller size than micro electromechanical system (MEMS), are promising to improve abilities of measuring small displacements and forces at a molecular scale. Meanwhile, nanomechanical resonator (NAMR) with sufficient high oscillation frequency at low temperature is supposed to behave as quantized harmonic oscillator. Due to their comparative sizes and energy scales as well as low dissipation, the coupling of NAMR and superconducting qubits has attracted a lot of interest to realize a novel solid-state cavity QED architecture. With this architecture, NAMR can serve as a data bus for multi-qubits operations of flux qubits. Coupling mechanism between flux qubit and NAMR also enables production and detection of quantum states of NAMR. However, existing theoretical investigations only concentrated on the coupling of NAMR with Josephson charge qubit while experimentally the coherence of flux qubit is undergoing rapid development.

We thus proposed an active mechanism to couple the mechanical motion mode of a NAMR to the persistent current in the loop of superconducting Josephson junction (or phase slip) flux qubit [1]. As shown in Fig.1, the coupling can be controlled *in situ* by an external classical magnetic field. According to our numerical estimation, the whole system forms a new solid-state cavity QED architecture in "strong coupling limit". This architecture can be used to demonstrate quantum optics phenomena as well as coherently manipulate the qubit for quantum information processing. The coupling mechanism is applicable for more generalized situations where the superconducting Josephson junction system is a multi-level system.

[1] F. Xue, Y. D. Wang, C. P. Sun, H. Okamoto, H. Yamaguchi, and K. Semba, New J. Phys. **9** (2007) 35.

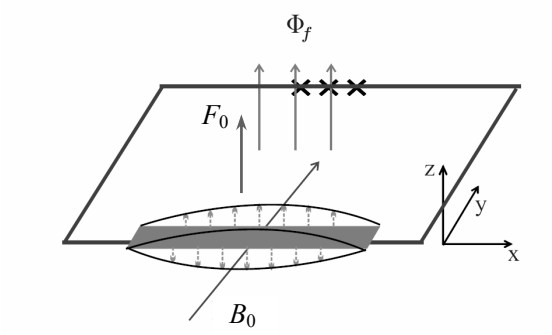

Fig. 1. A mechanical beam (the gray bar) is incorporated in a superconducting loop of a 3-Josephson-junction (each Josephson junction is indicated by a cross) flux qubit. Under a magnetic field B_0 along y direction, the persistent super-current in the qubit loop produces Lorentz force F_0 on the beam (NAMR) along z direction. Therefore, the z-direction motion of the beam is coupled with the persistent current of flux qubit.

10 GHz Clock Quantum Cryptography Experiment

Hiroki Takesue[1], Eleni Diamanti[2], Carsten Langrock[2], Martin M. Fejer[2], and Yoshihisa Yamamoto[2]
[1]Optical Science Laboratory, [2]Stanford University

For realizing practical quantum cryptography systems, increasing a key generation rate is important. Here we report a high-speed quantum cryptography experiment at a 10-GHz clock frequency [1] using frequency up-conversion detectors (UCD) [2] with improved timing jitter.

We employed differential phase shift quantum key distribution protocol [3]. An actively mode-locked laser output a 10-GHz clock pulse train whose wavelength and pulse width were 1551 nm and 10 ps, respectively. The phase of each pulse was randomly modulated by 0 or π. Then, the pulse train was attenuated so that the average photon number per pulse becomes 0.2, and transmitted over optical fiber. The output pulses from the fiber were launched into a 1-bit delayed interferometer, which was followed by two UCDs. In an UCD, a signal photon was combined with a 1319-nm pump light and injected into a PPLN waveguide, in which the signal photon was up-converted to a 700-nm photon. After suppressing noise photons with optical filters, the up-converted photon was detected by a low-jitter Si APD. With those detectors, we were able to receive high-speed photon trains with a high timing resolution.

Figure. 1 shows the histogram of detected signal when 3-ps pulses were input into an UCD. Although the full width at half maximum of the timing jitter was as small as 30 ps, a large tail was observed. We then adjusted the quantum efficiency, combined dark count rate, and time window width at 0.3%. 750 cps, and 10 ps, and undertook quantum key distribution. The sifted key rate at 100 km was 3.7 kbit/s. The obtained error rate as a function of fiber length is shown with squares in Fig. 2. The error rate was around 10%, which was due to the tailing characteristics of jitter. Interestingly, we did not observe significant variation in the error rate when we used fibers with different lengths. This indicates that the use of short pulses and narrow time window improved the ratio between signal and dark counts per time slot. Circles in Fig. 2 show estimated error rate due to dark counts. A dark count-induced error rate was suppressed to less then 1% even after 100 km transmission. Therefore, we can expect significant improvement in the error rate by improving the UCD timing jitter characteristics.

[1] H. Takesue, et al., Opt. Express **14** (2006) 9522.
[2] C. Langrock, et al., Opt. Lett. **30** (2005) 1725.
[3] K. Inoue, E. Waks, and Y. Yamamoto, Phys. Rev. Lett. **89** (2002) 037902.

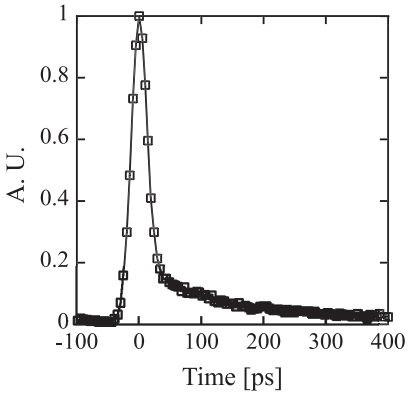

Fig.1. Detection signal histogram.

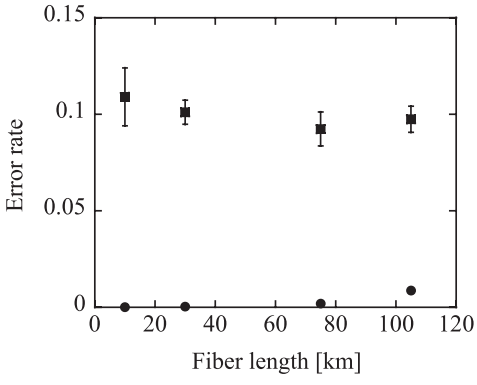

Fig. 2. Error rate as function of fiber length.

Differential-phase Quantum Key Distribution Experiment Using a Series of Quantum Entangled Photon Pairs

Toshimori Honjo[1], Hiroki Takesue[1], and Kyo Inoue[2]
[1]Optical Science Laboratory, [2]Osaka University/NTT Research Professor

Quantum key distribution (QKD) has been studied as a way to realize unconditionally secure communications. We had been intensively worked on differential-phase-shift QKD (DPS-QKD) experiment where randomly phase-modulated coherent pulse stream was used. Recently, we made a step toward more sophisticated QKD experiment using entangled photon pairs[1].

Figure 1 shows the experimental setup. A 1-GHz pulse stream amplified by an erbium-doped fiber amplifier (EDFA) was launched into a 500-m DSF. The DSF was cooled with liquid nitrogen to suppress noise photons through the spontaneous Raman scattering process. A series of time-correlated entangled photon pairs was generated in the DSF by the spontaneous four-wave mixing process[2]. After suppressing residual pump, the photons were input into an arrayed waveguide grating (AWG) that separated the signal and idler photons. The signal and idler photons were sent to Alice and Bob, respectively. Alice and Bob randomly imposed phase-modulation on the incoming pulses by 0 or $\pi/2$, and then launched them into 1-bit delay planar lightwave circuit (PLC) Mach-Zehnder interferometers. Setting the phase difference between the two arms to 0 and focusing on a certain time slot, they can obtain the following correlation

$$\left|\psi_f\right\rangle = \frac{1}{2\sqrt{2}}\{(e^{i(\theta_a+\theta_b)}+1)\left|A1\right\rangle\left|B1\right\rangle - (e^{i(\theta_a+\theta_b)}+1)\left|A2\right\rangle\left|B2\right\rangle - i(e^{i(\theta_a+\theta_b)}-1)\left|A1\right\rangle\left|B2\right\rangle - i(e^{i(\theta_a+\theta_b)}-1)\left|A2\right\rangle\left|B1\right\rangle\}$$

where θ_a and θ_b represents the differential phases imposed by Alice and Bob, respectively, $\left|wn\right\rangle$ represents the state that a photon goes to detector *n* placed at the output of each PLC Mach-Zehnder interferometer at site *w*, with *w*=*A*(Alice)or *B*(Bob). After the photon transmission, Alice and Bob disclosed the photon detection time and the differential phase imposed on corresponding pulses through a public channel. In cases that Alice and Bob detected photons at an identical time slot, they created a key bit using the above correlations.

With this setup, we generated sifted keys with a quantum bit error rate of 8.3 % and a sifted key generation rate of 0.3 bit /sec[3]. We revealed the feasibility of this QKD scheme, and showed the first step toward sophisticated quantum communications.

[1] K. Inoue, Phys. Rev. A **71** (2005) 032301.
[2] H. Takesue and K. Inoue, Opt. Express **13** (2005) 7832.
[3] T. Honjo, H. Takesue, and K. Inoue, Opt. Lett. **32** (2007) 1165.

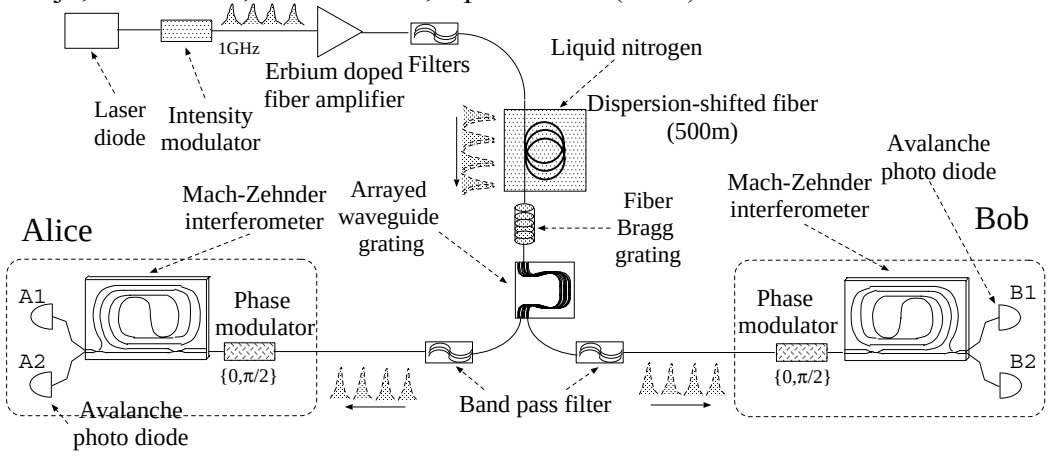

Fig. 1. Experimental setup.

Pair-wise Entanglement for Characterizing Quantum Phase Transition

Kaoru Shimizu and Akira Kawaguchi*
Optical Science Laboratory

Quantum behaviors of a one-dimensional interacting spin system have attracted many research interests because that offers some important theoretical models for condensed matter physicist. Moreover, from the view of one-way quantum computation, study of the spin system may provide a variable knowledge for designing its operation scheme. In particular, it is most important for us to establish a physically-clear interpretation for the variety of the behaviors that are regulated by quantum uncertainty depending on the different values of spin-spin interaction coefficient J and external magnetic field h.

By adapting some knowledge of quantum entanglement to the one-dimensional spin system, we here obtained an insight that the quantum behaviors of the system can be characterized in a quantitative way by small numbers of parameters; amplitudes and phases of four different types of quantum correlation (four Bell-states) between neighboring two spins, though the system is composed of many numbers of spins. We employed the one-dimensional anti-ferromagnetic Ising spin model represented by the Hamiltonian: $H=J\Sigma S^Z_i S^Z_{i+1}+h^x\Sigma S^Z_i$ with the transverse magnetic field h^x. Then we studied the behavior of pair-wise quantum entanglement† with regarding the different values of h/J, where the system changes from the random phase of S^Z_j (for a large h^x value) to the ordered phase (anti-ferromagnetic phase for a small h^x value). From critical behaviors of the pair-wise entanglement observed around the phase transition point, we can conclude that the amplitudes and phases of different quantum correlation provide a quantitative description of quantum spin fluctuation[1].

Our proposed method on the basis of the entanglement analysis is a useful tool for understanding the quantum behaviors of one or two dimensional spin systems.

[1] K. Shimizu and A. Kawaguchi, Phys. Lett. A **355** (2006) 176.

*Present address: Toyota Macs. Co. Ltd.

† Reduced density matrix ρ for the neighboring spins is decomposed into the separable part $(1-\Lambda)\rho_s$ and the inseparable part $\Lambda\rho_e$, (Fig.1) where ρ_e is decomposed into the four Bell states so (Fig.2) that $(1-\Lambda)$ is minimal. We employ concurrence $C(\rho)$ as a quantitative measure of pair-wise entanglement.

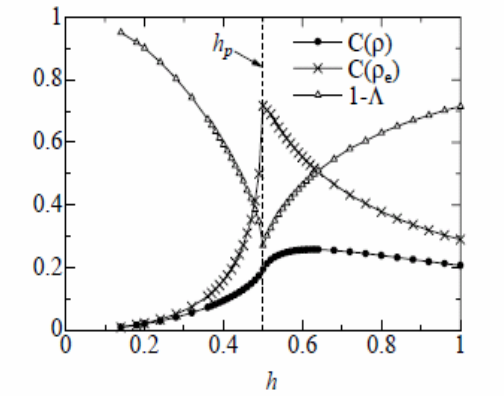

Fig.1. h dependence of concurrence $C(\rho)$ (h=0.5: phase transition point).

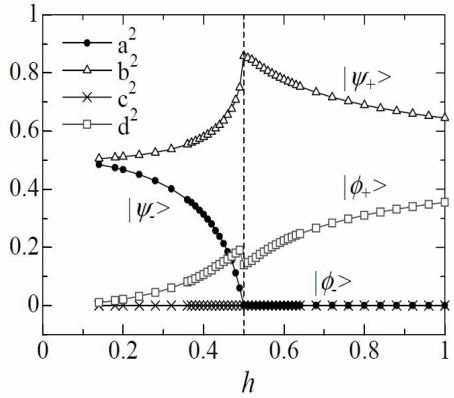

Fig.2. Decomposition of ρ_e into four Bell states (spin correlation).

Optical Properties of GaAs Quantum Dots Formed in (Al,Ga)As Nanowires

Haruki Sanada, Hideki Gotoh, Kouta Tateno, Tetsuomi Sogawa, and Hidetoshi Nakano
Optical Science Laboratory

Semiconductor nanowires (NWs) have been extensively investigated as fascinating candidates for nanoscale photonics and electronics applications. The vapor-liquid-solid (VLS) method is a technique for fabricating freestanding NWs with a broad range of semiconductor materials. The method not only produces one-dimensional structures, but also offers additional flexibility as regards band structure engineering by employing a conventional heterostructure technology. Here we report the results of an experimental photoluminescence (PL) measurement undertaken to clarify the optical properties of single GaAs quantum dots (QDs) formed in (Al,Ga)As NWs grown by the VLS method [1].

We fabricated GaAs QDs in (Al,Ga)As NW by the following two steps: (1) VLS growth of the NWs that have GaAs/(Al,Ga)As heterojunctions; and (2) normal MOVPE for covering the NWs with (Al,Ga)As cap layers, which suppress the non-radiative surface recombination of photoexcited carriers [2]. Figure 1 shows a cross-sectional SEM image of the similar structure composed of a GaAs/AlAs system instead of a GaAs/(Al,Ga)As system. The image shows that several QDs have formed inside the NW.

In Fig. 2, we compare the PL spectra with different excitation powers (P_{exc}) to examine the characteristics of the two peaks labeled by A and B. For $P_{exc} < 100$ W/cm^2, the integrated intensities of peak A and B have linear dependence with P_{exc} and P_{exc}^2, respectively, which is a typical behavior of exciton and biexciton emissions. In addition, the biexciton peak (peak B) energy exhibits a red shift and its linewidth broadens as P_{exc} increases. This might be a characteristic of QDs in NW structures grown by the VLS method because similar features have been reported in VLS-based InAs/GaAs and Ga(As,P)/GaP QDs systems. We also found that the PL depends on the optical polarization axis, indicating that the nanostructures have a highly asymmetrical shape. Although a more explicit consideration of their structural configurations is required to clarify the mechanism, our method is a promising way of engineering the positions and optical properties of GaAs/(Al,Ga)As nanostructures.

[1] H. Sanada, H. Gotoh, K. Tateno, and H. Nakano, Jpn. J. Appl. Phys. **46** (2007) 2578.
[2] K. Tateno, H. Gotoh, and Y. Watanabe, Appl. Phys. Lett. **85** (2004) 1808.

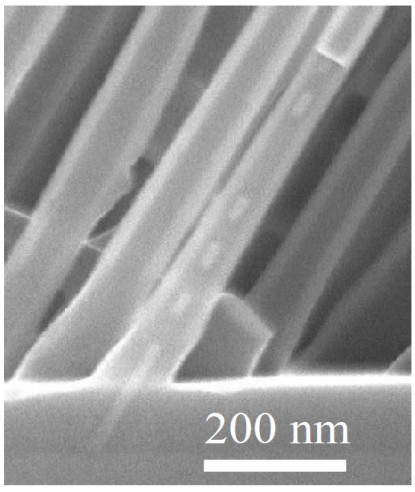

Fig. 1. Cross-sectional SEM image of dot-in-wire structure composed of a GaAs/AlAs system.

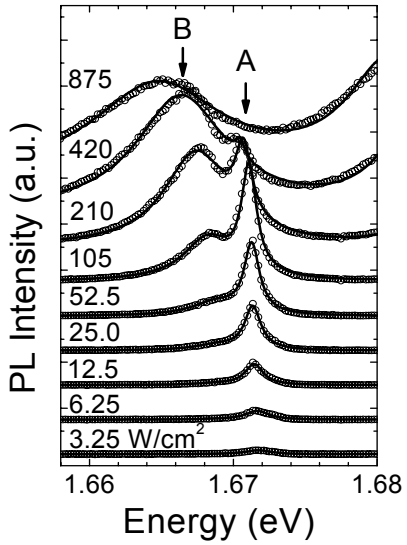

Fig. 2. Excitation power dependence of the PL spectra measured at 4 K.

Quantum Dot Laser Using Photonic Crystal Nanocavity

Takehiko Tawara[1], Hidehiko Kamada[1], Yong-Hang Zhang[2],
Takasumi Tanabe[1], and Tetsuomi Sogawa[1]
[1]Optical Science Laboratory, [2]Arizona State University

Photonic crystal (PhC) is advantageous for constructing nanocavities with a high quality factor (Q) and a wavelength-sized modal volume (Vm). A high Q/Vm nanocavity enhances the spontaneous emission rate of an active medium inside the cavity, and this enables us to produce optical devices with high efficiency and a low power consumption. Moreover, the use of semiconductor quantum dots (QDs) as an active medium will lead to higher efficiency owing to the suppression of phonon scattering and the surface recombination of carriers. Such QD PhC nanocavities are promising for use as ultrasmall and internal laser sources for photonic integrated circuits.

In general, QD PhC nanocavities have a III-V semiconductor heterostructure consisting of, for example, GaAs-based materials. However, in many cases the Q value was only several thousand, and this is insufficient to achieve the nanocavity effect. Certain factors are assumed to cause this problem; (i) the accuracy of the dry etching process is too low to obtain a high Q cavity, and (ii) there is a large optical loss induced by the re-absorption effect caused by QDs that are not coupled with the cavity mode.

To achieve high processing accuracy, we used EB lithographic resist as an etching mask and optimized the etching conditions for each layer with a different composition [1]. We also designed the PhC structure, including the materials composing it and the cavity mode detuning to the QD inhomogeneous broadening, to suppress the re-absorption effect. A Q of over 10,000 was achieved by making these improvements (Fig. 1) [2]. Moreover, a lasing action with very high spontaneous emission coupling to the lasing mode (β) was observed as a result of the excitation power dependence of the PL intensity and carrier lifetime (Fig. 2) [3].

These results provide us with a guideline for the structural design and fabrication method, and are important in terms of achieving highly efficient ultrasmall light sources.

[1] T. Tawara, et al., Jpn. J. Appl. Phys. Phys. **45** (2006) L917.
[2] T. Tawara, et al., IPRM2007, Matsue, Japan, May 2007.
[3] T. Tawara, et al., CLEO/QELS2007, Baltimore, USA, May 2007.

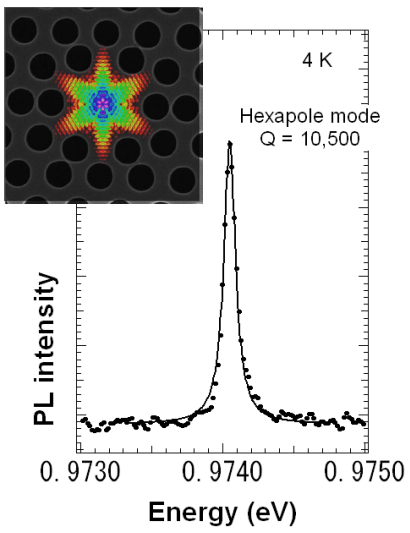

Fig. 1. Quantum dot emission via cavity mode.

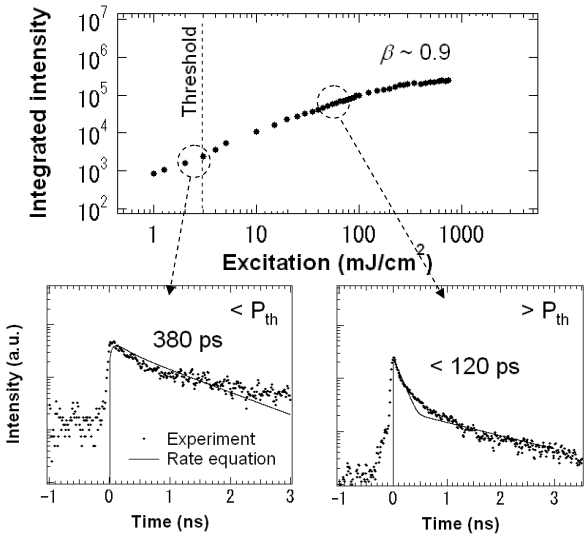

Fig. 2. Lasing characteristics.

Spatiotemporally Resolved Soft X-Ray Absorption Spectroscopy of a Femtosecond Laser Ablation Plume

Katsuya Oguri, Yasuaki Okano, Tadashi Nishikawa, and Hidetoshi Nakano
Optical Science Laboratory

Time-resolved x-ray measurement techniques have attracted much attention as a result of the recent progress on the ultrashort x-ray pulse generation technology based on laser-based x-ray sources and synchrotron radiation sources. These techniques enable us to measure the ultrafast dynamics of crystal structures, atomic distances, coordination numbers, and electronic states in a highly nonequilibrium state, and they are expected to become a key technique for the new interdisciplinary field linking conventional x-ray science and ultrafast optical science, namely "ultrafast x-ray science" [1].

We developed a spatiotemporally resolved XAS system by improving our previous time resolved XAS system [2]. Using the system, we measured the space and time evolution of a plume generated by the femtosecond-laser-ablation process, which is expected to become a new laser-processing technique [3]. We demonstrated that the system is a powerful tool for probing the complicated phenomenon that evolves temporally and spatially with the solid to liquid to gas phase transition, and the dissociation of chemical bonding [4].

The most noteworthy characteristic of our system is that it combines the short pulse duration of femtosecond laser plasma soft x-rays and the high spatial resolution of the Kirkpatrick-Baez microscope, thus considerably improving the temporal and spatial resolution, and the soft x-ray flux on a sample. The soft x-ray microscope and a transmission grating simultaneously provide us with spectral information and one-dimensional spatial information of an expanding laser ablation plume (Fig. 1). Figure 2 shows the temporal evolution of a spatially resolved absorbance spectrum for an Al ablation plume induced by 100-fs laser irradiation with an intensity of 1.5×10^{14} W/cm^2. This figure clearly shows that the Al ablation plume expands from the Al tape surface toward the vacuum with time. The most remarkable feature of the ablation plume is the significant shift of the $L_{II,III}$ absorption edge towards a shorter wavelength compared with that of solid Al. Since the wavelength of the $L_{II,III}$ absorption edge of the ablation plume corresponds to the transition energy from the 2*p* state to continuum states, the edge shift depends on each particle constituting the ablation plume. This result demonstrates that our system is a powerful tool for measuring the dynamics of laser ablation plumes.

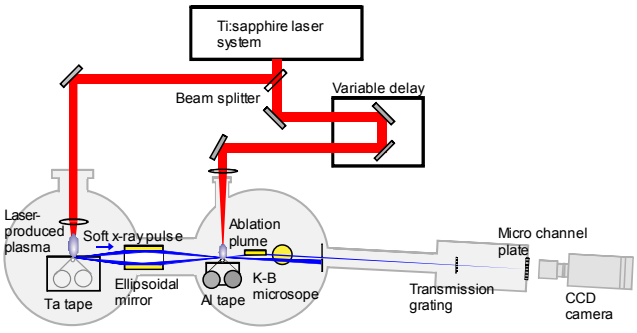

Fig. 1. Schematic illustration of the system.

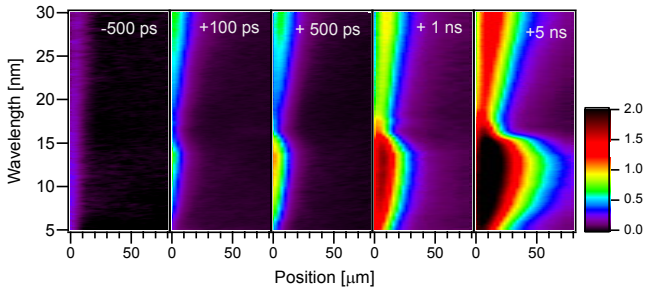

Fig. 2. Temporal evolution of spatially resolved absorbance spectrum for Al ablation plume.

[1] Bressler and Chergui, Chem. Rev. **104** (2004) 1781.
[2] Oguri, et al., Appl. Phys. Lett. **87** (2005) 011503.
[3] Okano, et al., Rev. Sci. Instrum. **77** (2006) 046105.
[4] Okano, et al., Appl. Phys. Lett. **89** (2006) 221502.

Time Resolved Measurement of Photonic Crystal Optical Nanocavity

Takasumi Tanabe, Eiichi Kuramochi, Akihiko Shinya,
Hideaki Taniyama, and Masaya Notomi
Optical Science Laboratory

A high-Q photonic crystal (PhC) nanocavity is very effective for application to all-optical switches that can operate at an ultra-low energy [1], because it can realize a high photon density at an extremely low input power. It is known that an ultra-high-Q can be achieved with a PhC nanocavity by employing the local width modulation of line defects [2]. A scanning electron microscope image of such a nanocavity is shown in Fig. 1 (a). Although it is difficult to recognize, the width of the line defect is slightly modulated in the circled region. As a result, a mode-gap cavity forms in this area. Indeed, the far-field pattern shows that the light is localized when the wavelength of the input light is same as the resonance of the cavity [Fig.1(b)]. Figure 1(c) shows the transmittance spectrum measured using a wavelength tunable laser. The transmittance width is an extremely small 1.3 pm, which corresponds to a Q of 1.2 million. To achieve higher wavelength resolution, we applied a single side band modulator to sweep the frequency of the laser light with an ultra-high accuracy. We obtained the same Q value and confirmed the accuracy of the measurement [3].

In contrast, since an ultra-high Q cavity system has a long photon lifetime, the Q can be directly obtained in the time domain. In addition, time resolved measurement is a powerful way to characterize the dynamic behavior of the cavity system. Therefore, we combined ring-down measurement with time correlated single photon counting to obtain the optical property of the PhC cavity in the time domain [4]. First, a rectangular pulse is employed as the input, and it is suddenly turned off at 0 ns. Then the photons that where trapped in the cavity start to decay through the output waveguide. By observing the discharging signal using time resolved measurement we obtained a photon lifetime of 1.01 ns [Fig. 2(a)]. The accuracy and the reproducibility of time domain measurement were confirmed [5] and the photon lifetime agrees perfectly with that obtained with spectral domain measurement.

Finally we studied the propagation of a pulse through the cavity system by using time resolved measurement. We obtained a pulse delay of 1.45 ns for an input pulse with a width of 1.9 ns [Fig. 2(b)]. This value corresponds to the record smallest group velocity of 5.8 km/s demonstrated in any dielectric slow-light material. The above result paves the way for the application of the enhancement of light and matter interaction or the development of an optical delay line with a small footprint.

[1] T. Tanabe, et al., Appl. Phys. Lett. **90** (2007) 031115.
[2] E. Kuramochi, et al., Appl. Phys. Lett. **88** (2006) 041112.
[3] T. Tanabe, et al., Electron. Lett. **43** (2007) 187.
[4] T. Tanabe, et al., Nat. Photonics **1** (2007) 49.
[5] T. Tanabe, et al., Opt. Express **15** (2007) 7816.

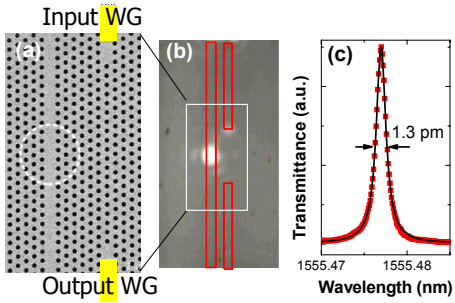

Fig. 1. (a) Scanning electron microscope image of a width-modulated line defect PhC nanocavity. (b) Far field pattern of the resonant light. (c) Transmittance spectrum.

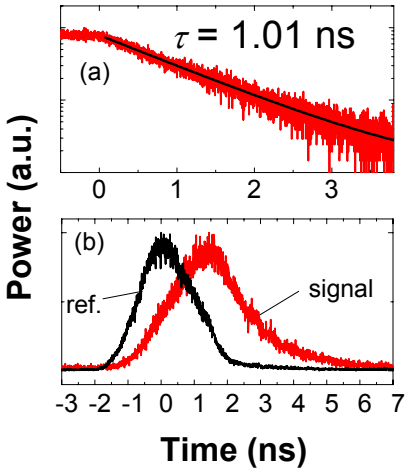

Fig. 2. (a) Discharging waveform. (b) Pulse response.

Coupled Resonator Waveguides Formed by Ultrahigh-*Q* Si Photonic Crystal Nano-resonators

Eiichi Kuramochi, Takasumi Tanabe, Hideaki Taniyama, and Masaya Notomi
Optical Science Laboratory

A periodic chain of optical resonators (coupled resonator optical waveguide: CROW) has been expected as a promising candidate of a slow light media [1]. An ultrahigh intrinsic quality factor (Q) of a resonator is required to achieve ultraslow group velocity (v_g) and low propagation loss simultaneously. Recently, we have demonstrated that such CROW is achievable on a Si photonic crystal (PC) platform besides an advantage of ultra-small footprint (~3μm@single resonator.)

Figure 1(a) is a microscope image of a PC-CROW fabricated by electron beam lithography (the number of the resonator: N=3.) A locally width-modulated line-defect resonator [2] realized ultrahigh experimental Q (1.2×10^6)[3]. Sharp peaks which corresponded to CROW modes were clearly observed in transmittance measurements (Fig. 1(b).) Figure 2 shows dispersion of CROW modes when the interval of the resonator (L_{CC}) was 7a (a: lattice constant=420nm.) Surprisingly, the dispersion of the coupled resonator modes were fitted well by almost equal theoretically derived cosine-function, which corresponded to very small coupling coefficient κ (~7×10^{-4}), when N was changed from 5 to 60. The passing of light over 60 PC resonators was achieved for the first time which successfully demonstrated advantage of ultrahigh-Q. The dispersion was controlled well by L_{CC} (Fig. 3) and the lowest κ (3.3×10^{-4}) corresponded to very slow v_g (~5×10^{-3}c; c: the speed of light in vacuum.)

This work is encouraging possibility of a PC-based CROW as a slow light media.

[1] A. Yariv, et al., Opt. Lett. **24** (1999) 711.
[2] E. Kuramochi, et al., Appl. Phys. Lett. **88** (2006) 041112.
[3] T. Tanabe, et al., Opt. Express. **15** (2007) 7826.

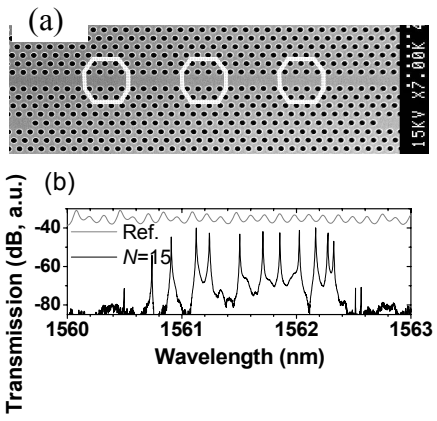

Fig. 1. (a) Microscope image of a PC-CROW (N=3, L_{CC}=9a.) The white octagons show modified holes which creates ultrahigh-Q resonators (The parameter is described in Ref. 3.) (b) A transmission spectrum of a PC-CROW (L_{CC}=7a, N=15).

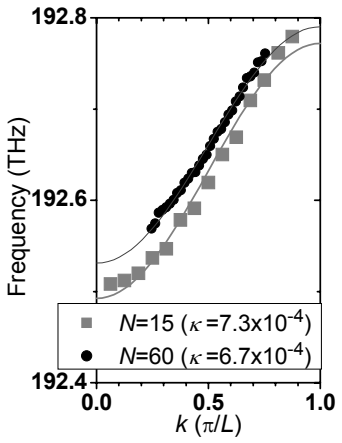

Fig. 2. Dispersion characteristics of PC-CROWs (L_{CC}=7a).

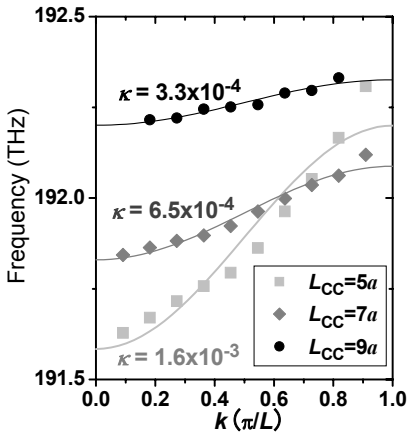

Fig. 3. Dispersion characteristics of PC-CROWs (N=10).

Optical Micromachine by Ultrahigh-Q Nanocavities

Masaya Notomi and Hideaki Taniyama
Optical Science Laboratory

Recently, ultrahigh-Q and simultaneously ultra-small optical cavities have been realized by photonic crystals [1]. In such ultrahigh-Q nanocavities, various light-matter interactions are expected to be greatly enhanced. We have theoretically found that we can convert optical energies into mechanical energies extremely efficiently by employing specially-designed photonic-crystal nanocavities [2]. Our result demonstrates that one can introduce mechanical displacement by extremely weak light, and indicates possibilities towards ultra-efficient optical micro-machines in future.

Figure 1 shows our sample structure, which is a point defect cavity of a double-layer photonic crystal. It is practically the same as our ultrahigh-Q photonic-crystal cavity design except an air slit is inserted in the center of the slab. This cavity is special because one can largely change the resonant wavelength by slight change of the slab spacing (slit width) without deteriorating cavity Q. Owing to this feature, an optical pulse captured in this cavity can generate extraordinary large radiation force (~ 1 μN per 1 pJ), because this force is determined by the spatial derivative of the electromagnetic energy in the cavity. Furthermore, this large force can do a large mechanical work due to the long cavity photon lifetime. Consequently, the optical energy of the optical pulse is converted to the mechanical energy very efficiently. We calculated this efficiency assuming realistic parameters, as shown in Fig. 2. Generally, such opto-mechanical energy conversion is intrinsically very inefficient ($\sim 10^{-12}$) because of the mass-less nature of light (except photon rockets having relativistic speed). Figure 2 shows that the efficiency can reach up to 10%. Such extremely-high efficiency is only possible for mechanical displacement incorporated to ultrahigh-Q and ultrasmall cavities.

When the optical energy is converted to mechanical, the frequency of light in the cavity is lowered. In other words, one can realize wavelength conversion of light using the reverse process. Our numerical calculation shows that large wavelength conversion (larger than 20% of the original wavelength) is indeed possible. Last year, we have reported that adiabatic wavelength conversion is possibly by dynamically tuning the resonance frequency of a cavity [3]. In fact, the present opto-mechanical process is physically identical. That is, very efficient optical micromachines are intrinsically very efficient opto-mechanical wavelength converters.

[1] E. Kuramochi, et al., Appl. Phys. Lett. **88** (2006) 041112.
[2] M. Notomi, et al., Phys. Rev. Lett. **97** (2006) 023903.
[3] M. Notomi, et al., Phys. Rev. A**73** (2006) 051803(R).

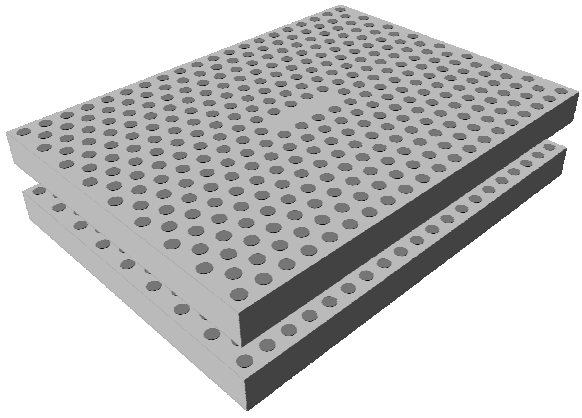

Fig. 1. Double-layer photonic crystal cavity.

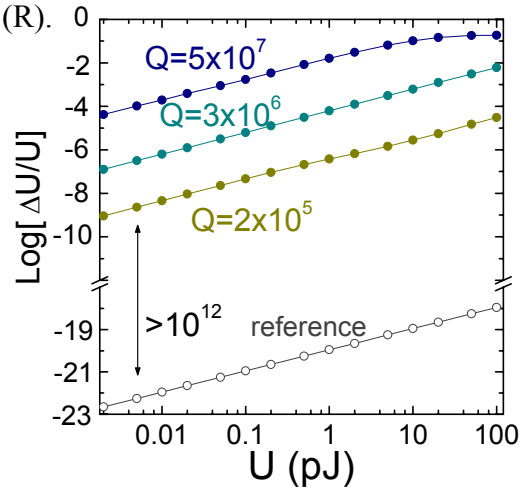

Fig. 2. Energy conversion efficiency.

Ⅱ. Data

The 4th Advisory Board

The Advisory Board, an external committee whose role is to evaluate the work of NTT Basic Research Laboratories (BRL), met from February 6 - 8, 2007. This was the fourth meeting of the Advisory Board, which was first convened in 2001 to provide an objective evaluation of our research plans and activities to enable us to employ strategic management in a timely manner. On this occasion, we were happy to welcome a new member.

Over the course of the three days the board made valuable suggestions and comments in relation to our research and management activities. They commented that the research level is generally high on an international scale, and that it is important for us to maintain this top-level research and transmit information about our research achievements to the world. They also raised several issues related to human resources, the research budget and internal and external collaboration. We plan to make improvements based on these valuable suggestions.

At this meeting we offered both young researchers and NTT executives an opportunity to communicate with the board members. This included a lunch party for young researchers at which they were able to interact with the board members. For the NTT executives, we organized a Japanese style dinner, which provided a good chance to discuss the future management strategy of NTT BRL from an international perspective. The next board meeting will held in eighteen months.

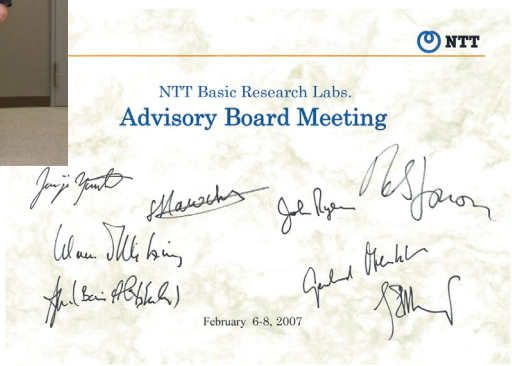

Board members	Affiliations	Research fields
Prof. Abstreiter	Walter Shottky	Low-dim. physics
Prof. Altshuler	Columbia Univ.	Condensed matter
Prof. Haroche	Ecole Normale	Quantum optics
Prof. Jonson	Chalmers UT	Condensed matter
Prof. Leggett	Univ. Illinois	Quantum physics
Prof. Mooij	Delft UT	Quantum computer
Prof. Ryan	Univ. Oxford	Nano-bio technology
Prof. von Klitzing	Max-Planck-Inst.	Semiconductor physics

International Conference on Nanoelectronics, Nanostructures and Carrier Interactions

The international conference on nanoelectronics, nanostructures and carrier interactions (NNCI2007) was held from February 21 to 23, 2007, at the NTT Atsugi R&D Center in collaboration with *Solution Oriented Research for Science and Technology* (SORST) sponsored by the *Japan Science and Technology Agency* (JST).

Ultra-small "nano-scale" structures and the behavior of carriers in these structures have been the focus of a lot of attention for many years. Recently, the field has been advanced significantly through the introduction of additional degrees of freedom, such as electron and nuclear spin, magnetism, and mechanical motion. In addition, novel quantum mechanical concepts such as quantum computing and quantum cryptography are attracting a great deal of interest. With the aim of further advancing these studies, this conference aspired to gather leading scientists and provide forum for discussing the most recent topics in nanoelectronics, nanostructures, and carrier interactions. The conference was chaired by Dr. Toshimasa Fujisawa and Dr. Hiroshi Yamaguchi of NTT Basic Research Laboratories, together with Prof. Yoshiro Hirayama of Tohoku University.

On February 21, after the opening and welcoming remarks by Dr. Junji Yumoto, Director of NTT Basic Research Laboratories, the technical session was opened with the plenary talk "Architecture for a Shor Factorization Engine Based on Semiconductor Spins" by Prof. E. Yablonovitch from University of California, Los Angeles. There were 17 oral presentations on coherent spin control, quantum information processing, 2-dimensional systems, metal-insulator transition, and electron transport in quantum dots, and 20 poster presentations. On the 22nd, the 15 oral presentations discussed nanowires and nanotubes, novel heterostructures, spintronics, and novel spin materials, and 20 posters were presented. On the 23rd, there were 15 oral presentations on scanning probe spectroscopy and imaging, electron correlation and interference, silicon nanoelectronics, and spin-related phenomena in nanostructures. We believe that we provided a very nice opportunity for mutual communication within and among the related research fields.

The participants were totally 145 people. All participants well enjoyed the high-quality presentations and discussions on nanoelectronics, nanostructures, and carrier interactions.

Award Winners' List (Fiscal 2006)

Minister of MEXT (Ministry of Education, culture, sports, science, and technology) Young Scientist Award	A. Fujiwara	"Physics and device application of nanostructures in the field of semiconductors"	Apr. 18, 2006
35th Annual International Symposium on Multiple-Valued Logic (ISMVL-2005) Outstanding Paper Award	K. Degawa T. Aoki T. Higuchi H. Inokawa Y. Takahashi	"A Two-Bit-per-Cell Content-Addressable Memory Using Single-Electron Transistors"	May 19, 2006
The Laser Society of Japan 26th Annual Meeting Best Paper Award	T. Tanabe	"All-optical switching and 5-GHz RZ (Return to Zero) optical pulse train modulation using silicon photonic crystal cavities"	May 31, 2006
European Materials Research Society (E-MRS) 2006 Spring Meeting Best Poster Presentation	H. Omi	"Strain and Thermal Stability of Thin Silicon Overlayers on and between SiO_2"	June 2, 2006
IEED/LEOS Distinguished Lecturer Award	M. Notomi	"All-Optical Control of Photonic Crystals"	July 1, 2006

JJAP Award for the Best Original Paper	S. Horiguchi A. Fujiwara H. Inokawa Y. Takahashi	"Analysis of Back-Gate Voltage Dependence of Threshold Voltage of Thin Silicon-on-Insulator Metal-Oxide-Semiconductor Field-Effect Transistor and Its Application to Si Single-Electron Transistor"	Aug. 29, 2006
The Japan Society of Applied Physics Young Scientist Award for the Presentation of Excellent Paper	T. Tanabe	"Direct time domain measurement of photon lifetime for ultra-high-Q photonic crystal optical nanocavities"	Mar. 27, 2007

In-house Award Winners' List (Fiscal 2006)

NTT R&D Award	K. Muraki N. Kumada	"Techniques for precise control of nuclear spins using semiconductor nanostructures"	Feb.15, 2007
NTT R&D Award	Y. Taniyasu M. Kasu T. Makimoto	"AlN deep-ultraviolet light-emitting diode with 210-nm wavelength"	Feb.15, 2007
Award for Achievements by Director of Basic Research Laboratories	Y. Taniyasu M. Kasu T. Makimoto	"Development of technologies for AlN crystal growth, doping, and light-emitting device"	Mar.22, 2007
Award for Achievements by Director of Basic Research Laboratories	K. Nishiguchi Y. Ono A. Fujiwara H. Inokawa	"Room-temperature operation of single-electron transfer and detection using Si transistors"	Mar.22, 2007
Award for Excellent Papers by Director of Basic Research Laboratories	T. Fujisawa	"Bidirectional counting of single electrons" Science Vol. 312, 1634 (2006).	Mar.22, 2007
Award for Excellent Papers by Director of Basic Research Laboratories	A. Nishikawa K. Kumakura	"High critical electric field of AlGaN p-i-n vertical conducting diodes on n-SiC substrate" Appl. Phys. Lett. Vol. 88, 173508 (2006).	Mar.22, 2007
Award for Excellent Papers by Director of Basic Research Laboratories	H. Takesue T. Honjo	"Differential phase shift quantum key distribution experiment over 105km fibre" New J. Phys. Vol. 7, 232 (2005).	Mar.22, 2007
Special Award by Director of Basic Research Laboratories	Y. Harada	"The contribution to the new collaboration researches scheme in U.K. "	Mar.22, 2007

List of Visitors' Talks (Fiscal 2006)

I. Materials Science

Date	Speaker	Affiliation "Topic"
May 29	Dr. Michael Jetter	University of Stuttgart, Germany "Quantum dots for single photon applications"
May 29	Mr. Sarad Bahadur Thapa	University of Ulm, Germany "Structural and spectroscopic properties of AlN layers grown by MOVPE"
June 6	Dr. Eric Mueller	Coherent Inc. "Continuous-Wave THz Transceivers & CW Coherent High-Dynamic-Range THz Imaging"
July 7	Dr. Goo-Hwan Jeong	CREST Honma Project "Diameter control and functionalization of carbon nanotubes"
Sep. 7	Prof. Wolfgang Stolz	Philipps-University, Germany "Novel dilute nitride III/V-semiconductor laser system for the integration to Si-microelectronics"
Sep. 15	Prof. Erhard Kohn	University of Ulm, Germany "Diamond electronics will it be able to compete with III-Nitrides? "
Oct. 6	Mr. Toshiaki Kato	Tohoku University "Vertically aligned growth of single walled carbon nanotubes by plasma-enhanced CVD and its plasma effects"
Oct. 6	Mr. Ken Okada	Tohoku University "Functionalization of single walled carbon nanotubes by DNA"
Oct. 26	Prof. Etienne Bustarret	CNRS-LEPES, France "Superconducting B-doped diamond and related materials: recent progress"
Feb. 1	Dr. Taisuke Ohta	E. O. Lawrence Berkeley National Laboratory, U.S.A. "Controlling the Electronic Structure of Graphene Layers"

II. Physical Science

Date	Speaker	Affiliation "Topic"
May 16	Prof. Kiyofumi Muro	Chiba University "High-sensitive and high-resolution spectroscopy of spin quasi-phase and spin dynamics in semiconductor nanostructure at low temperature and in high magnetic field"
July 12	Dr. Koji Usami	Tokyo Institute of Technology "On Quantumness of Collective Spin Excitation"
Aug. 1	Dr. Sebastian Hofferberth	University of Heidelberg "Radio-frequency dressed state potentials for neutral atoms"
Aug. 11	Dr. Jens Hefort	Paul Drude Institute, Germany "Expitaxial Heusler alloys on GaAs substrates"
Aug. 29	Mr. Tomohiro Tanaka	University of Tokyo "Phase Information from Two–Terminal Conductance of Quantum Dot Systems"
Sep. 5	Prof. Mikio Eto	Keio University "Spin injection through semiconductor quantum point contact"
Sep. 11	Dr. Kasper Grove-Rasmussen	Niels Bohr Institute, Denmark "Electronic transport in Carbon Nanotubes with normal and superconducting leads"
Sep. 12	Prof. Klaus Ploog	Paul Drude Institute, Germany "Ferromagnetic Semiconductors for Spin Injection"
Sep. 14	Prof. Yukio Tanaka	Nagoya University "Odd-frequency pairing state in superconducting junctions"
Oct. 20	Mr. Toshiyuki Ihara	University of Tokyo "Photoluminescence and photoluminescence excitation spectra of one-dimensional electron systems in T-shaped quantum wires"
Oct. 26	Dr. Romain Danneau	University of New South Wales, Australia "Spin related phenomena in ballistic hole quantum wires"
Nov. 6	Prof. Alec Maassen van den Brink	Riken

		"Four-qubit superconducting quantum circuit"
Jan. 22	Prof. Yasser Omar	Technical University of Lisbon, Portugal "Generation of Entanglement in Quantum Wire and Application to Single-Electron Transmittivity"
Jan. 29	Prof. Michel H. Devoret	Yale University, U.S.A. "Quantum-mechanical electrical circuits"
Jan. 30	Prof. Michel H. Devoret	Yale University, U.S.A. "Measurement of Dynamical Casimir Effect"
Jan. 31	Prof. Michel H. Devoret	Yale University, U.S.A. "Quantum Voting"
Feb. 1	Prof. Michel H. Devoret	Yale University, U.S.A. "QND fraction of JBA readout"
Feb. 9	Prof. Hans Mooij	Delft University of Technology, Netherlands "Quantum Information Processing Using Superconducting Circuit"
Feb. 16	Dr. Fei Xue	Riken "Liquid-State NMR Based Quantum Computing & Cavity Quantum Electrodynamics in Solid-State System"
March 15	Prof. Lev B. Ioffe	The State University of New Jersey, U.S.A. "Microscopic origin of low frequency noises in Josephson qubits"
March 15	Dr. Lara Faoro	The State University of New Jersey, U.S.A. "The challenge of error correction in quantum computation"

III. Optical Science

Date	Speaker	Affiliation "Topic"
Apr. 11	Dr. Kouichi Ichimura	Toshiba Corporation "EIT in a solid system and its application to quantum information Processing"
July 3	Prof. See Leang Chin	Laval University, Canada "Some new applications using femtosecond laser filamentation in air"
Aug. 21	Dr. Michael Stopa	Harvard University, U.S.A. "Magnetic field control of exchange and noise immunity in double quantum dots"

Oct. 23	Dr. Sergei Studenikin	National Research Council of Canada, Canada "Role of magnetoplasmons in microwave induced resistance oscillations and zero-resistance states"
Nov. 27	Prof. Norbert Lutkenhaus	University of Waterloo, Canada "Security key rates, upper bounds and limitations in quantum key distribution"
Dec. 4	Prof. Daniel Gottesman	Perimeter Institute for Theoretical Physics, Canada "The threshold for fault-tolerant quantum computation"
Dec. 6	Dr. Sae Woo Nam	National Institute of Standards and Technology, U.S.A. "Superconducting detectors for quantum information applications"
Dec. 22	Dr. Hiroaki Terashima	Tokyo Institute of Technology "Relativistic Effects on the Einstein-Podolsky-Rosen Correlation"
Jan. 9	Prof. Shun-Lien Chuang	University of Illinois, U.S.A. "Slow Light in Quantum Dots and Quantum Wells"
March 2	Prof. Ora Entin-Wohlman	Ben Gurion University, Israel "The magnetic structure of lanthanum titanate"
March 13	Prof. Robert M. Westervelt	Harvard University, U.S.A. "Imaging Electrons in Nanoscale Devices"

Research Activities of Basic Research Laboratories in 2006

The numbers of research papers, presentations at the international conferences and applied patents amounted to 169, 254, and 52 in Basic Research Laboratories as a whole. All numbers according their research areas are as follows.

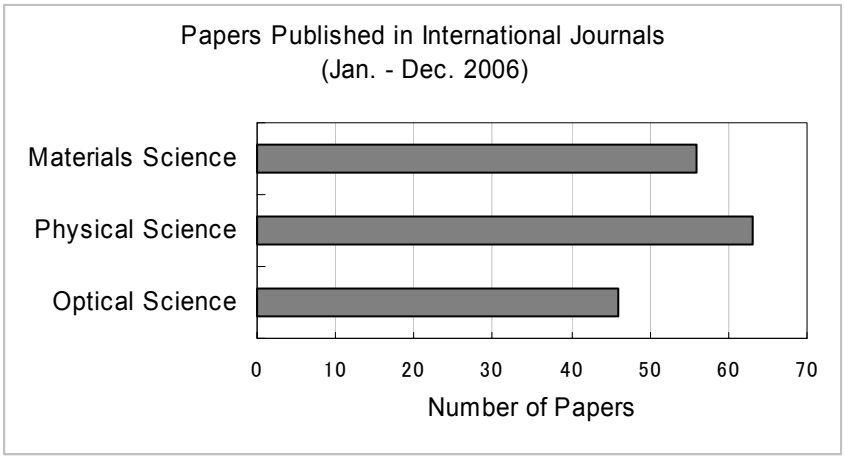

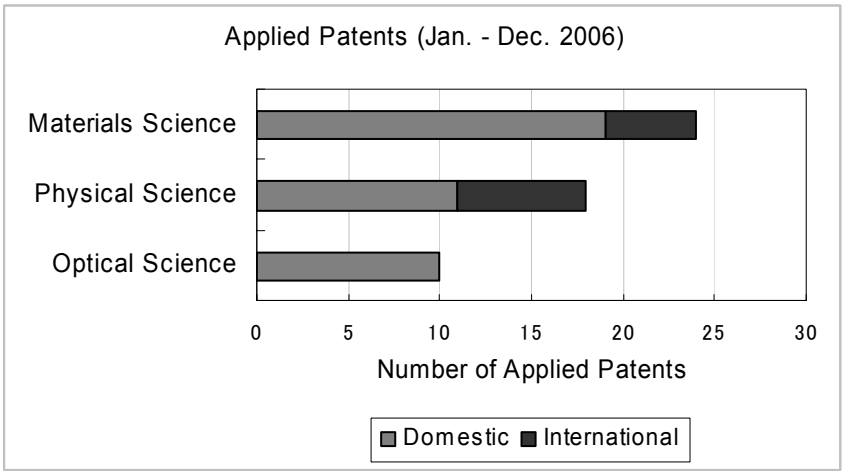

The numbers of research papers published in the major journals are shown below.

General Science Journals

Journal titles	(IF2006)*	numbers
Science	(30.927)	3
Nature	(29.273)	1

Specialized Science Journals

Journal titles	(IF2006)*	numbers
Applied Physics Letter	4.127	21
Japanese Journal of Applied Physics	1.096	18
Physical Review B	3.185	11
Physica E	0.946	10
Physical Review Letters	7.489	9
Journal of Applied Physics	2.498	9
Optics Express	3.764	7
Physical Review A	2.997	7
Chemical Physics Letters	2.438	4
Diamond and Related Materials	1.988	4
Physica B	0.796	4
IEEE Electron Device Letters	2.825	3
Physica C	0.948	3
Nano Letters	9.847	1
Reports on Progress in Physics	8.893	1

*IF2006: Impact Factor 2006（Journal Citation Reports, 2006）

The average IF2006 for all research papers from NTT Basic Research Laboratories is 3.26.

The numbers of presentations in the major conferences are shown below.

Conference titles	numbers
28th International Conference on Physics of Semiconductors (ICPS28)	21
2006 International Conference on Soliid State Devices and Materials (SSDM2006)	21
International Symposium on Mesoscopic Superconductivity and Spintronics 2006 (MS+S2006)	19
Conference on Lasers and Electro-Optics Quantum Electronics and Laser Science Conference / Quantum Electronics and Laser Science Conference (CLEO/QELS)	9
7th International Conference on the Science and Application of Nanotubes (NT06)	8
Frontiers in Nanoscale Science and Technology (FNST2006)	8
14th International Conference on Molecular Beam Epitaxy (MBE2006)	7
International Workshop on Nitride Semiconductors (IWN2006)	7
International Conference on Nanoscience and Technology (ICN+T2006)	6
12th Conference on Laser Optics (LO2006)	6
2006 Materials Research Society Fall Meeting (MRS 2006 Fall)	5
IEEE Lasers and Electro-Optics Society 19th Annual Meeting (LEOS2006)	5
1st Canada－Japan SRO-COAST Symposium on Ultrafast Intense Laser Science	4
19th International Symposium on Superconductivity (ISS2006)	4
VIth Recontre de Vietnam, Nanophysics: from Fundamentals to Applications	3
International Symposium on Ultrafast Intense Laser Science (ISUILS5)	3
International Symposium on Compound Semiconductors (ISCS2006)	3
International Conference on Raman Spectroscopy (ICORS2006)	3
American Chemical Society, 232nd National Meeting and Exposition (ACS)	3
2006 International Workshop on Dielectric Thin Films for Future ULSI Devices-Science & Technology (IWDTF2006)	3
2006 IEEE Silicon Nanoelectronics Workshop (SNW2006)	3

List of Invited Talks at International Conferences (2006)

I. Materials Science Laboratory

(1) H. Omi, "Step Pattern Formation during Molecular Beam Epitaxy", Symposium on Surface Physics 2006, Shizukuishi, Japan (Jan. 2006).

(2) H. Hibino and M. Uwaha, "Instability of Steps During Ga Deposition on Si(111) ", Symposium on Surface Physics 2006, Shizukuishi, Japan (Jan. 2006).

(3) H. Miyashita, I. Fujimoto, K. Hamada, K. Mikoshiba, and K. Torimitsu, "A High-Speed AFM Observation of Inositol 1,4,5-Trisphosphate Receptor Reconstituted into a Lipid Bilayer.", VIII. Annual Linz Winter Workshop, Linz, Austria (Feb. 2006).

(4) K. Ajito, "Laser-trapping Raman Spectroscopy of Neurotransmitters in Single Nerve Terminals", The 6th France-Japan Workshop on Nanomaterials, Sapporo, Japan (Mar. 2006).

(5) M. Kasu, "Diamond RF Power Transistors: Present Status and Prospects", Materials Congress 2006, London, U.K. (Apr. 2006).

(6) Y. Taniyasu, M. Kasu, and T. Makimoto, "Formation Mechanism of Threading Dislocations in AlN during MOVPE Growth", 13th International Conference on Metal Organic Vapor Phase Epitaxy (ICMOVPE-XIII), Miyazaki, Japan (May 2006).

(7) K. Torimitsu, "NanoBioscience –Analysis of Neural Functions with Bio-Molecules–", 7th International Conference "Materials in Clinical Applications" of the Forum on New Materials, Sicily, Italy (Jun. 2006).

(8) K. Ajito, R. Rungsawang, I. Tomita, and Y. Ueno, "Near-Infrared Raman and Terahertz Spectroscopy and Biological Molecule Imaging", 20th International Conference on Raman Spectroscopy (ICORS), Yokohama, Japan (Sep. 2006).

(9) M. Kasu, K. Ueda, Y. Yamauchi, A. Tallaire, and T. Makimoto "Diamond-Based RF Power Transistors: Fundamentals and Applications", The 17th European Conference on Diamond, Diamond-Like Materials, Carbon Nanotubes, Nitrides and Silicon Carbide (Diamond 2006), Estoril, Portugal (Sep. 2006).

(10) K. Torimitsu, "Neurons and Receptor Proteins for Nano-Bio Interface", The Nano-Bio-Cogno Convergence Seminar 2006: Valorization in Medicine and Healthcare (SOC-45), Leuven, Belgium (Sep. 2006).

(11) H. Omi, "Step Instabilities on Vicinal Si(111) during Molecular Beam Epitaxy", 1st non-virtual meeting "Instabilities at Surfaces", Burgas, Bulgaria (Sep.-Oct. 2006).

(12) Y. Taniyasu, M. Kasu, and T. Makimoto, "AlN deep-UV LEDs with a Wavelength of 210 nm", 6th Akasaki Research Center Symposium, Nagoya, Japan (Oct. 2006).

(13) K. Torimitsu, "Role of Magnesium in Neural Process", 11th International Magnesium Symposium, Ise-Shima, Japan (Oct. 2006).

(14) M. Kasu, K. Ueda, A. Tallaire, Y. Yamauchi, and T. Makimoto, "Diamond Transistors for RF Power Applications", Kobe University Frontier Technology Forum –Nano- and Photonics-Technology in Innovation–, Kobe, Japan (Nov. 2006).

II. Physical Science Laboratory

(1) T. Mukai, "Quantum Computation with Atoms: Practical Schemes and Problems", Post-COE Workshop on Cold Atoms: Fermion and Optical Lattice, Kyoto, Japan (Feb. 2006).

(2) H. Takayanagi, S. Sasaki, S. Kang, S. Miyashita, T. Maruyama, H. Tamura, T. Akazaki, and Y. Hirayama, "Manipulation and Control of Spins in III-V Semiconductors by Gated Structures", 2006 RCIQE International Seminar, Sapporo, Japan (Feb. 2006).

(3) Y. Ono, A. Fujiwara, K. Nishiguchi, Y. Takahashi, and H. Inokawa, "Single-Electron Transfer in Silicon: Towards Single-Dopant Electronics", 3rd International Workshop on Ubiquitous Knowledge Network Environment, Sapporo, Japan (Feb.-Mar. 2006).

(4) K. Semba, "Coherent Control of a Flux-Qubit Coupled to a Quantum LC-Resonator", UNI Erlangen Winter Seminar on Superconductivity, Finkenberg, Austria (Mar. 2006).

(5) T. Fujisawa, "Counting Statistics of Single-Electron Transport through a Double Quantum Dot", Capri Spring School on Transport in Nanostructures, Capri, Italy (Apr. 2006).

(6) Y. Ono, K. Nishiguchi, K. Takashina, H. Inokawa, S. Horiguchi, and Y. Takahashi, "Impurity Conduction and its Control in SOI MOSFETs; Towards Silicon Single-Dopant Electronics", 2006 IEEE Silicon Nanoelectronics Workshop (SNW2006), Honolulu, Hawaii, U.S.A. (Jun. 2006).

(7) T. Fujisawa, "Counting Statistics of Single Electron Transport through a Double Quantum Dot", IEEE Nanotechnology Materials and Devices Conference

(IEEE-NMDC2006), Daejeon, Korea (Jun. 2006).

(8) Y. Hirayama, "Single-Electron Manipulation and Detection in a Quantum Dot System", International Conference for Quantum Structure Science (ICQS-2006), Beijing, China (Jun. 2006).

(9) K. Semba, J. Johansson, S. Saito, T. Meno, H. Tanaka, H. Nakano, M. Ueda, and H. Takayanagi, "Vacuum Rabi Oscillations Observed in a Flux Qubit LC-Oscillator System", Macroscopic Quantum Coherence and Computing (MQC2), Napoli, Italy (Jun. 2006).

(10) M. Uematsu, "Oxygen Self-Diffusion in Silicon Dioxide: Effect of the Si/SiO_2 Interface", 2nd International Conference on Diffusion in Solid and Liquids (DSL2006), Aveiro, Portugal (Jul. 2006).

(11) G. Yusa, K. Muraki, N. Kumada, K. Takashina, K. Hashimoto, and Y. Hirayama, "Nuclear Spin Control by a Point Contact", 28th International Conference on Physics of Semiconductors (ICPS28), Vienna, Austria (Jul. 2006).

(12) K. Suzuki, K. Kanisawa, S. Perraud, M. Ueki, K. Takashina, and Y. Hirayama, "Observation of Subband Standing Waves in Superlattices by Low-Temperature Scanning Tunneling Spectroscopy", 28th International Conference on Physics of Semiconductors (ICPS28), Vienna, Austria (Jul. 2006).

(13) H. Takayanagi, S. Saito, J. Johansson, H. Tanaka, H. Nakano, M. Ueda, and K. Semba, "Flux Qubit Coupled to an LC-Resonator", Materials and Mechanisms of Superconductivity High Temperature Superconductors VIII (M2S-HTSC-VIII), Dresden, Germany (Jul. 2006).

(14) K. Muraki, "Interaction of Electron and Nuclear Spins in Quantum Wells", 17th International Conference on High Magnetic Fields in Semiconductor Physics (HMF-17), Wuerzburg, Germany (Jul.-Aug. 2006).

(15) Y. Hirayama, "High Precision Control of Nuclear Spins in Semiconductor Nanostructures", 13rd International Conference on Superlattice, Nanostructures and Nanodevices (ICSNN-2006), Istanbul, Turkey (Jul.-Aug. 2006).

(16) T. Fujisawa, "Counting Statistics of Single Electron Transport through a Double Quantum Dot", VIth Recontre de Vietnam, Nanophysics: from Fundamentals to Applications, Hanoi, Vietnam (Aug. 2006).

(17) Y. Hirayama, S. Sasaki, and T. Fujisawa, "Non-Local Charge and Spin Interactions in Semiconductor Quantum Dot Systems", International Workshop "Tera- and Nano-Devices: Physics and Modeling", Aizu-wakamatsu, Japan (Aug. 2006).

(18) G. Yusa, K. Muraki, N. Kumada, K. Takashina, K. Hashimoto, and Y. Hirayama, "Controlled Multiple Quantum Coherences of Nuclear Spins", 4th International Conference on Physics and Application of Spin-Related Phenomena in Semiconductors (PASPS-IV), Sendai, Japan (Aug. 2006).

(19) K. Semba, J. Johansson, S. Saito, T. Meno, H. Tanaka, H. Nakano, M. Ueda, and H. Takayanagi, "Vaccum Rabi Oscillations Observed in a Flux Qubit LC-Oscillator System", VIth Recontre de Vietnam, Nanophysics: from Fundamentals to Applications, Hanoi, Vietnam (Aug. 2006).

(20) H. Nakano, "Some theoretical aspects in Superconducting Flux-qubit systems", VIth Recontre de Vietnam, Nanophysics: from Fundamentals to Applications, Hanoi, Vietnam (Aug. 2006).

(21) H. Takayanagi, T. Akazaki, S. Yanagi, and H. Munekata, "Transport Properties of Ferromagnetic Semiconductors with Superconducting Electrodes", International Workshop on Mesoscopic Superconductivity and Magnetism (MesoSuperMag 2006), Chicago, U.S.A. (Aug.-Sep. 2006).

(22) K. Muraki, "Spin/Charge Fluctuations in Quantum Hall Bilayers -Nuclear Spin Relaxation and Coulomb Drag", Interactions, Excitations and Broken Symmetries in Quantum Hall Systems (QHSyst-06), Dresden, Germany (Oct. 2006).

(23) K. Semba, "Josephson Junction Qubits", 2006 US-Japan Workshop on Quantum Information Science, Hawaii, U.S.A. (Oct. 2006).

(24) K. Semba, "Superconducting Flux Qubit Coupled to an LC-Oscillator", 19th International Symposium on Superconductivity (ISS2006), Nagoya, Japan (Oct.-Nov. 2006).

(25) H. Takayanagi, Y.-L. Zhong, and T. Akazaki, "Noise and Conductance Fluctuation due to Andreev Reflection", 19th International Symposium on Superconductivity (ISS2006), Nagoya, Japan (Oct.-Nov. 2006).

III. Optical Science Laboratory

(1) Y. Tokura, "Coherent Single Electron Spin Control in a Slanting Zeeman Field", A workshop on Imaging at the Nanoscale, Quantum Information Processing, Nanophotonics, Nanoelectronics: Frontiers in Nanoscale Science and Technology (FNST), San Francisco, U.S.A. (Jan. 2006).

(2) Y. Tokura, "Electron Spin Manipulation in Quantum Dot Systems", International Workshop on Electron Spin Resonance and Related Phenomena in Low Dimensional Structures, Sanremo, Italy (Mar. 2006).

(3) Y. Tokura, "Interaction and Interference Effect in the Electron Current through Laterally Coupled Quantum Dots", International Seminar and Workshop on Non-equilibrium Dynamics in Interacting Systems, Dresden, Germany (Apr. 2006).

(4) Y. Tokura, "Coherent Transport through Coupled Quantum Dots", MTI & CNM International Argonne Fall Workshop on Nanophysics VI, Nanoscale Superconductivity and Magnetism, Argonne, France (Nov. 2006).

(5) M. Notomi, "Photonic Crystal Waveguides and Resonators", ePIXnet Winter School, Pontresina, Switzerland (Mar. 2006).

(6) M. Notomi, "Light Control by Photonic Crystals", ePIXnet Winter School, Pontresina, Switzerland (Mar. 2006).

(7) M. Notomi, E. Kuramochi, T. Tanabe, A. Shinya, and H. Taniyama, "All-Optical Control of Photonic Crystal Nanocavities", 2006 Optical Society of America Integrated Photonics Research and Applications Topical Meeting/ Nanophotonics Topical Meeting (OSA IPRA/NANO), Uncasville, U.S.A. (Apr. 2006).

(8) M. Notomi, T. Tanabe, E. Kuramochi, A. Shinya, H. Taniyama, and S. Mitsugi, "Dynamic Control of Light by Photonic-Crystal Resonator-Waveguide-Coupled System", Conference on Lasers and Electro-Optics/ Quantum Electronics and Laser Science Conference (CLEO/QELS'06), Long Beach, U.S.A. (May, 2006).

(9) H. Nakano, K. Oguri, Y. Okano, and T. Nishikawa, "Picosecond Time-Resolved XAFS Measurements Using Femtosecond Laser-Produced Plasma X-Rays as a Probe," XII International Conference on Laser Optics (LO'06), St. Petersburg, Russia (Jun. 2006).

(10) M. Notomi, E. Kuramochi, T. Tanabe, A. Shinya, and H. Taniyama, "All-Optical Control of Photonic Crystal Nanocavities", Journée Nationale Cristaux Photoniques, Marcoussis, France (Jun. 2006).

(11) H. Nakano, K. Oguri, Y. Okano, and T. Nishikawa, "Time-Resolved XAFS Measurements Using Femtosecond Laser-Produced Plasma X-Rays", 1st Canada-Japan SRO-COAST Symposium on Ultrafast Intense Laser Science, Tokyo, Japan (Jul. 2006).

(12) M. Notomi, E. Kuramochi, T. Tanabe, A. Shinya, and H. Taniyama, "All-Optical Control of Photonic Crystal Nanocavities", 11th OptoElectronics and Communications

Conference (OECC2006), Kaohsiung, Taiwan R.O.C. (Jul. 2006).

(13) M. Notomi, E. Kuramochi, T. Tanabe, A. Shinya, and H. Taniyama, "All-Optical Control Of Ultrasmall High-Q Photonic Crystal Nanocavities", Asia-Pacific Optical Communications Conference 2006 (APOC2006), Gwangju, Korea (Sep. 2006).

(14) S. Kawanishi, "High-Speed Optical Transmission Technology Using All-Optical Signal Processing", Asia-Pacific Optical Communications Conference 2006 (APOC2006), Gwangju, Korea (Sep. 2006).

(15) M. Notomi, E. Kuramochi, T. Tanabe, A. Shinya, and H. Taniyama, "All-Optical Switching and Dynamic Control of Light by Photonic Crystal Nanocavities", 2006 International Conference on Solid State Devices and Materials (SSDM2006), Yokohama, Japan (Sep. 2006).

(16) K. Yamada, T. Tsuchizawa, T. Watanabe, H. Fukuda, H. Shinojima, T. Tanabe, and S.-I. Itabashi, "All-Optical Signal Processing Using Nonlinear Effects in Silicon Photonic Wire Waveguides", The 19th Annual Meeting of the IEEE Lasers and Electro-Optics Society, (LEOS2006), Montreal, Canada (Oct.-Nov. 2006).

(17) H. Nakano, K. Oguri, Y. Okano, and T. Nishikawa, "Femtosecond Laser-Induced Melting and Ablation Processes Observed by Picosecond-Time-Resolved XAFS Using Femtosecond Laser-Produced Plasma Soft X-Ray Pulses", 5th International Symposium on Ultrafast Intense Laser Science (ISUILS5), Lijiang, China (Nov. 2006).

(18) K. Oguri, Y. Okano, T. Nishikawa, and H. Nakano, "Ejection of Liquid Aluminum Nanoparticles in Femtosecond-Laser-Ablation Plume Observed by Spatiotemporally-Resolved XAFS", 5th International Symposium on Ultrafast Intense Laser Science (ISUILS5), Lijiang, China (Nov. 2006).

(19) M. Notomi, "All-Optical Control of Photonic Crystals", Photonic Crystal Meeting of IEEE Lasers and Electro-Optics Society (LEOS) Scottish Chapter, St. Andrews, U.K. (Nov. 2006).

(20) A. Yokoo and H. Namatsu, "Nanoelectrode Lithography", 2006 Materials Research Society Fall Meeting (MRS 2006 Fall), Boston, U.S.A. (Nov.-Dec. 2006).

(21) M. Notomi, "All-Optical Control of Light in Photonic Crystals", 2006 Symposium of the IEEE Lasers and Electro-Optics Society (LEOS) Benelux Chapter, Eindhoven, The Netherlands (Dec. 2006).

NTT Basic Research Laboratories
3-1 Morinosato Wakamiya, Atsugi,
Kanagawa 243-0198, Japan
URL: http://www.brl.ntt.co.jp